Cell Reports
Article

Intertissue Control of the Nucleolus via a Myokine-Dependent Longevity Pathway

Fabio Demontis,[1,2,*] Vishal K. Patel,[1] William R. Swindell,[3] and Norbert Perrimon[1,4]
[1]Department of Genetics, Harvard Medical School, Boston, MA 02115, USA
[2]Division of Developmental Biology, Department of Developmental Neurobiology, St. Jude Children's Research Hospital, Memphis, TN 38105, USA
[3]Department of Dermatology, University of Michigan School of Medicine, Ann Arbor, MI 48109, USA
[4]Howard Hughes Medical Institute, Harvard Medical School, Boston, MA 02115, USA
*Correspondence: fabio.demontis@stjude.org
http://dx.doi.org/10.1016/j.celrep.2014.05.001

SUMMARY

Recent evidence indicates that skeletal muscle influences systemic aging, but little is known about the signaling pathways and muscle-released cytokines (myokines) responsible for this intertissue communication. Here, we show that muscle-specific overexpression of the transcription factor Mnt decreases age-related climbing defects and extends lifespan in *Drosophila*. *Mnt* overexpression in muscle autonomously decreases the expression of nucleolar components and systemically decreases rRNA levels and the size of the nucleolus in adipocytes. This nonautonomous control of the nucleolus, a regulator of ribosome biogenesis and lifespan, relies on Myoglianin, a myokine induced by Mnt and orthologous to human GDF11 and Myostatin. *Myoglianin* overexpression in muscle extends lifespan and decreases nucleolar size in adipocytes by activating p38 mitogen-activated protein kinase (MAPK), whereas Myoglianin RNAi in muscle has converse effects. Altogether, these findings highlight a key role for myokine signaling in the integration of signaling events in muscle and distant tissues during aging.

INTRODUCTION

Aging is characterized by changes in multiple organ systems that collectively decrease the ability of the organism to withstand homeostatic perturbations (Kenyon, 2010). Depending on the tissue considered, tissue-specific activation of longevity pathways can result in only local effects (i.e., prevention of tissue aging without systemic effects; Wessells et al., 2004) or also influence aging processes in other tissues via endocrine signals (Durieux et al., 2011; Giannakou et al., 2004; Hwangbo et al., 2004; Karpac et al., 2011; Libina et al., 2003; Rera et al., 2011; Satoh et al., 2013; Taguchi et al., 2007; van Oosten-Hawle et al., 2013; Wang et al., 2005, 2008). This network of tissue interactions has been proposed to coordinate the rate of aging of different tissues within an organism and regulate lifespan (Panowski and Dillin, 2009; Russell and Kahn, 2007). However, despite its importance, the key tissues and endocrine signals involved are only in part known.

Epidemiological studies in humans indicate that the mortality rate and pathogenesis of many age-related diseases are associated with sarcopenia and the functional status of skeletal muscle (Metter et al., 2002; Ruiz et al., 2008; Swindell et al., 2010). These findings suggest that the muscle is a key tissue with the capacity to influence systemic aging and lifespan (Demontis et al., 2013a, 2013b; Nair, 2005). In line with this hypothesis, several muscle-specific genetic interventions have been recently reported to extend lifespan in mice and in the fruit fly *Drosophila* (Demontis and Perrimon, 2010; Demontis et al., 2013a; Duteil et al., 2010; Gates et al., 2007; Hakimi et al., 2007; Katewa et al., 2012; Owusu-Ansah et al., 2013; Pospisilik et al., 2007). For instance, muscle-specific overexpression of uncoupling protein 1 (*UCP1*) in mice increases the median lifespan and decreases the incidence of several age-related pathologies arising in nonmuscle tissues, such as lymphomas, diabetes, and hypertension (Gates et al., 2007). Moreover, activation of the transcription factor FOXO and its target 4E-BP solely in skeletal muscles preserves muscle function, extends lifespan and prevents the gradual accumulation of polyubiquitin protein aggregates in muscles and other aging tissues via the autonomous and nonautonomous increase in basal autophagy in *Drosophila* (Demontis and Perrimon, 2010; Bai et al., 2013). Although these findings underscore the fundamental role of muscles in regulating systemic aging, the molecular mechanisms involved in this intertissue communication are largely unknown.

Over the past decade, skeletal muscle has been recognized as an endocrine tissue with the capacity to secrete several cytokines and growth factors, known as myokines, which can act on distant tissues such as the adipose tissue, liver, pancreatic β cells, and endothelium (Demontis et al., 2013a; Pedersen and Febbraio, 2012). For example, activity of the transcriptional coactivator peroxisome proliferator-activated receptor γ coactivator-1α (PGC-1α) in muscle protects from obesity and diabetes in mice at least in part via the induction of irisin, a myokine that promotes browning of white adipose tissues (Boström et al., 2012). Whether the emerging role of skeletal muscle in influencing systemic aging and lifespan depends on the action of myokines is largely unknown.

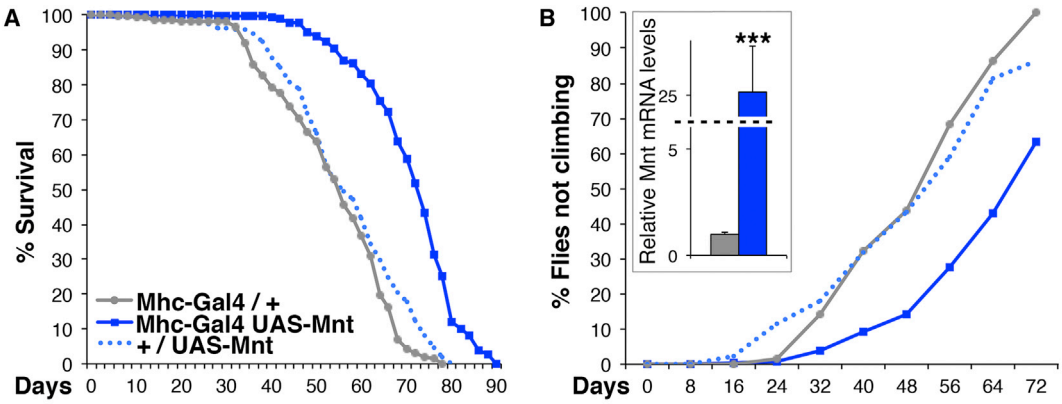

C *Microarray analysis (muscle)*

GO categories with decreased expression in response to Mnt transcriptional activity

GOCCID	P value	Odds Ratio	Exp Count	Count	Size	Term
GO:0005730	1.8522E-05	7.09157562	1.54652595	9	56	nucleolus
GO:0000313	0.00014265	5.27509653	1.9883905	9	72	organellar ribosome
GO:0005762	0.00134684	5.59246052	1.24274406	6	45	mitochondrial large ribosomal subunit
GO:0015934	0.00449461	3.35786469	2.6235708	8	95	large ribosomal subunit
GO:0005763	0.0446765	4.12237762	0.80087951	3	29	mitochondrial small ribosomal subunit

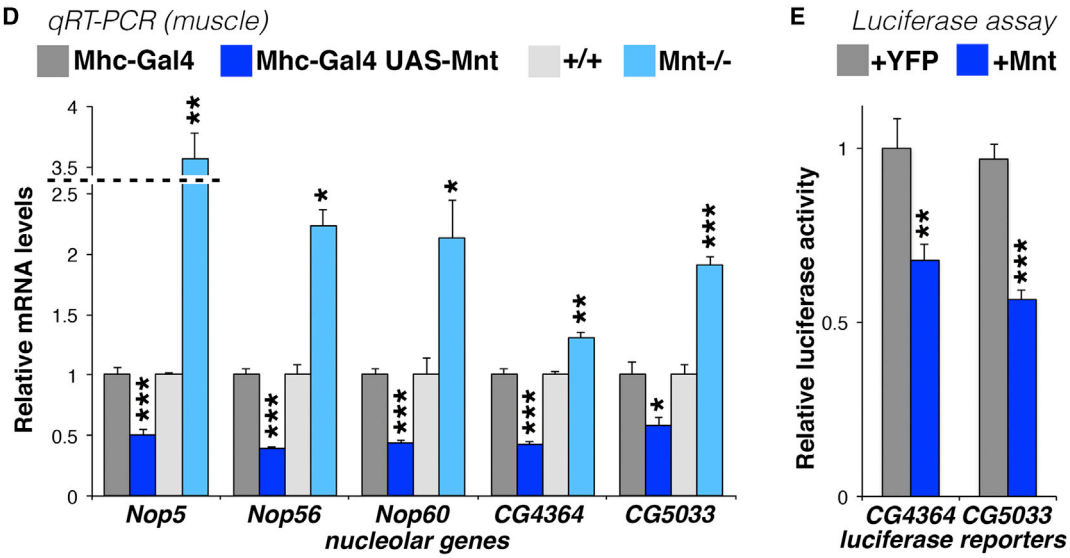

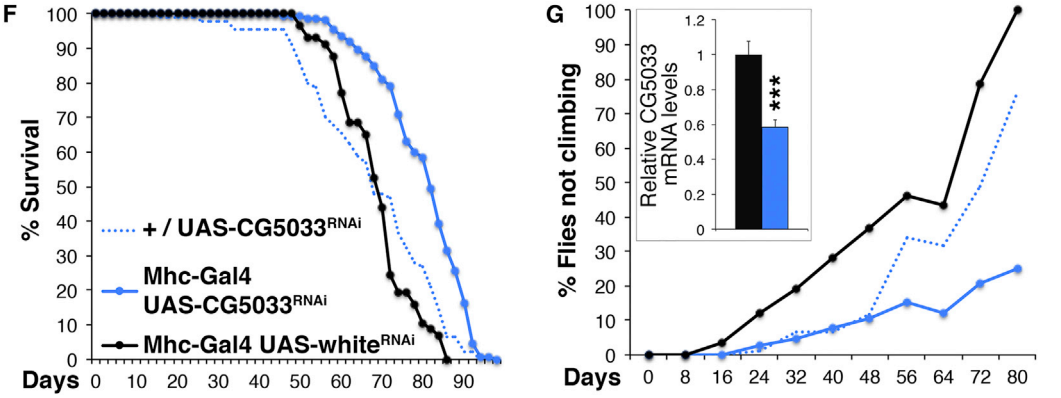

(legend on next page)

In this study, we found that overexpression of the transcription factor *Mnt* in skeletal muscle extends lifespan and regulates nucleolar function autonomously in muscle and nonautonomously in adipocytes. In muscle, Mnt decreases the expression of nucleolar components and rRNA levels and promotes the expression of *myoglianin*, a secreted protein homologous to human GDF11 and myostatin. In turn, overexpression of *myoglianin* in muscle leads to a systemic decrease in rRNA levels and reduces nucleolar size in adipocytes by activating the stress-sensing kinase p38 mitogen-activated protein kinase (MAPK). Altogether, these findings indicate a key role for myokine signaling in the intertissue regulation of aging.

RESULTS

Mnt Activity in Skeletal Muscle Decreases the Expression of Nucleolar Components and Extends Lifespan

Drosophila Mnt is a basic helix-loop-helix transcription factor homologous to human MNT/MAD that decreases the growth and proliferation of epithelial cells by directly regulating the expression of several target genes involved in ribosome biogenesis and cellular anabolism (Hurlin and Huang, 2006; Orian et al., 2005). Although *Mnt* null flies are short-lived (Loo et al., 2005), the role of Mnt in aging is not understood. In *Drosophila*, Mnt protein is detected in the nuclei of several tissues, including skeletal muscle of adult flies (Figure S1). To test whether muscle-restricted overexpression of *Mnt* regulates lifespan, we used the Mhc-Gal4 driver, which has been previously shown to drive transgene expression specifically in skeletal muscle but not in nonmuscle tissues (Demontis and Perrimon, 2010; Schuster et al., 1996). We crossed the skeletal-muscle-specific *Mhc-Gal4* line with either males carrying a *UAS-Mnt* transgene or isogenic siblings having the same genetic background but no transgene and analyzed the resulting progenies (*Mhc-Gal4/+* and *Mhc-Gal4/UAS-Mnt*). We also analyzed heterozygous *+/UAS-Mnt* flies as additional controls. *Mnt* overexpression in skeletal muscle extended both the median and maximum lifespan (Figure 1A), and this effect was not associated with changes in muscle mass, body weight, or feeding behavior, as assessed with capillary feeding (CAFE) assays (Figure S2 and data not shown). We next used negative geotaxis assays to test whether Mnt regulates age-related muscle functional decay and found that *Mnt* overexpression in muscle lowers the percentage of flies with climbing defects during aging (Figure 1B). Lifespan extension and preservation of climbing ability was also obtained by inducing *Mnt* overexpression with the dMef2-Gal4 driver under control of the temperature-sensitive $Gal80^{ts}$ (Figure S3).

To examine the transcriptional changes induced by Mnt in skeletal muscle, we profiled gene expression changes with Affymetrix microarrays. Gene ontology cell-component terms most significantly downregulated by *Mnt* overexpression included ribosomal proteins and components of the nucleolus (Figure 1C), a nuclear compartment necessary for ribosome subunit biogenesis (Dimario, 2004), suggesting that the nucleolus is a key effector of Mnt in lifespan regulation. Quantitative RT-PCR (qRT-PCR) confirmed a decrease in the expression of genes encoding nucleolar components (*Nop5*, *Nop56*, *Nop60*, *CG4364*, and *CG5033*) in *Mnt*-overexpressing muscles, whereas muscles from $Mnt^{-/-}$ null flies showed an increase in the expression of these genes (Figure 1D). Luciferase assays in *Drosophila* S2R+ cells with reporters based on the promoters of *CG4364* and *CG5033* further confirmed this regulation (Figure 1E).

The nucleolus has been linked with the regulation of replicative senescence in yeast (Guarente, 1997) and is emerging as a key cellular hub for stress sensing in multicellular organisms (Boulon et al., 2010; Mayer et al., 2005; Michel et al., 2011). Interventions that delay cellular aging and extend lifespan, such as rapamycin, AMP-activated protein kinase activity, and decreased target of rapamycin signaling, are known to reduce the size and function of the nucleolus (Grewal et al., 2007; Hoppe et al., 2009; Iadevaia et al., 2012; Zhang et al., 2000). On this basis, we next tested whether the nucleolus is per se a determinant of lifespan acting

Figure 1. *Mnt* Overexpression in Skeletal Muscle Extends Lifespan and Decreases Age-Related Muscle Dysfunction and Nucleolar Protein Gene Expression

(A and B) *Mnt* overexpression in skeletal muscle extended the median and maximum lifespan (A; *Mhc-Gal4/UAS-Mnt*; blue; n = 311; median/maximum lifespan = 72.4/90 days; $p < 0.0001$) and reduced the percentage of flies with age-related climbing defects (B; $p < 0.001$; log-rank test) as compared with isogenic control siblings (*Mhc-Gal/+*; gray; n = 257; median/maximum lifespan = 54.8/78 days) and heterozygous UAS-transgene-alone controls (*+/UAS-Mnt*; blue dotted line; n = 236; median/maximum lifespan = 55.7/80 days). Relative *Mnt* mRNA levels are shown in the inset with n = 4 and SEM indicated; ***$p < 0.001$; unpaired two-tailed Student's t test.

(C) Gene expression profiling of skeletal muscle overexpressing *Mnt* and controls with Affymetrix microarrays. Genes encoding components of the nucleolus and the ribosome are significantly represented among the target genes having decreased expression in response to Mnt transcriptional activity ($p < 0.05$; Exp Count, expected count).

(D) Relative mRNA levels of nucleolar components from skeletal muscles with increased Mnt levels, from $Mnt^{-/-}$ null flies, and controls. *Mnt* overexpression (dark blue) decreased the mRNA levels of nucleolar components as compared with controls (dark gray). Conversely, *Mnt* loss of function (blue) led to increased expression. SEM is indicated with n = 4; unpaired two-tailed Student's t test.

(E) *Mnt* overexpression (blue) decreased the activity of luciferase reporters based on the promoters of the *CG4364* and *CG5033* genes (which encode nucleolar components) as compared with controls (*YFP* overexpression; gray). SEM is indicated with n = 16.

In (D) and (E), *$p < 0.05$; **$p < 0.01$; ***$p < 0.001$; unpaired two-tailed Student's t test.

(F and G) *CG5033* RNAi in skeletal muscle extended the median lifespan (F; *Mhc-Gal4/UAS-CG5033^{RNAi}*; blue; n = 152; median/maximum lifespan = 81.9/98; $p < 0.0001$; log-rank test) and reduced the percentage of flies with age-related climbing defects (G; $p < 0.01$; log-rank test) as compared with a mock RNAi treatment against *white* (*Mhc-Gal/UAS-white^{RNAi}*; black; n = 57; median/maximum lifespan = 68.6/86) and heterozygous UAS-transgene-alone controls (*+/UAS-CG5033^{RNAi}*; blue dotted line; n = 90; median/maximum lifespan = 67.7/94). Relative *CG5033* mRNA levels are shown in the inset with n = 4 and SEM indicated; ***$p < 0.001$; unpaired two-tailed Student's t test.

See also Figures S1–S3.

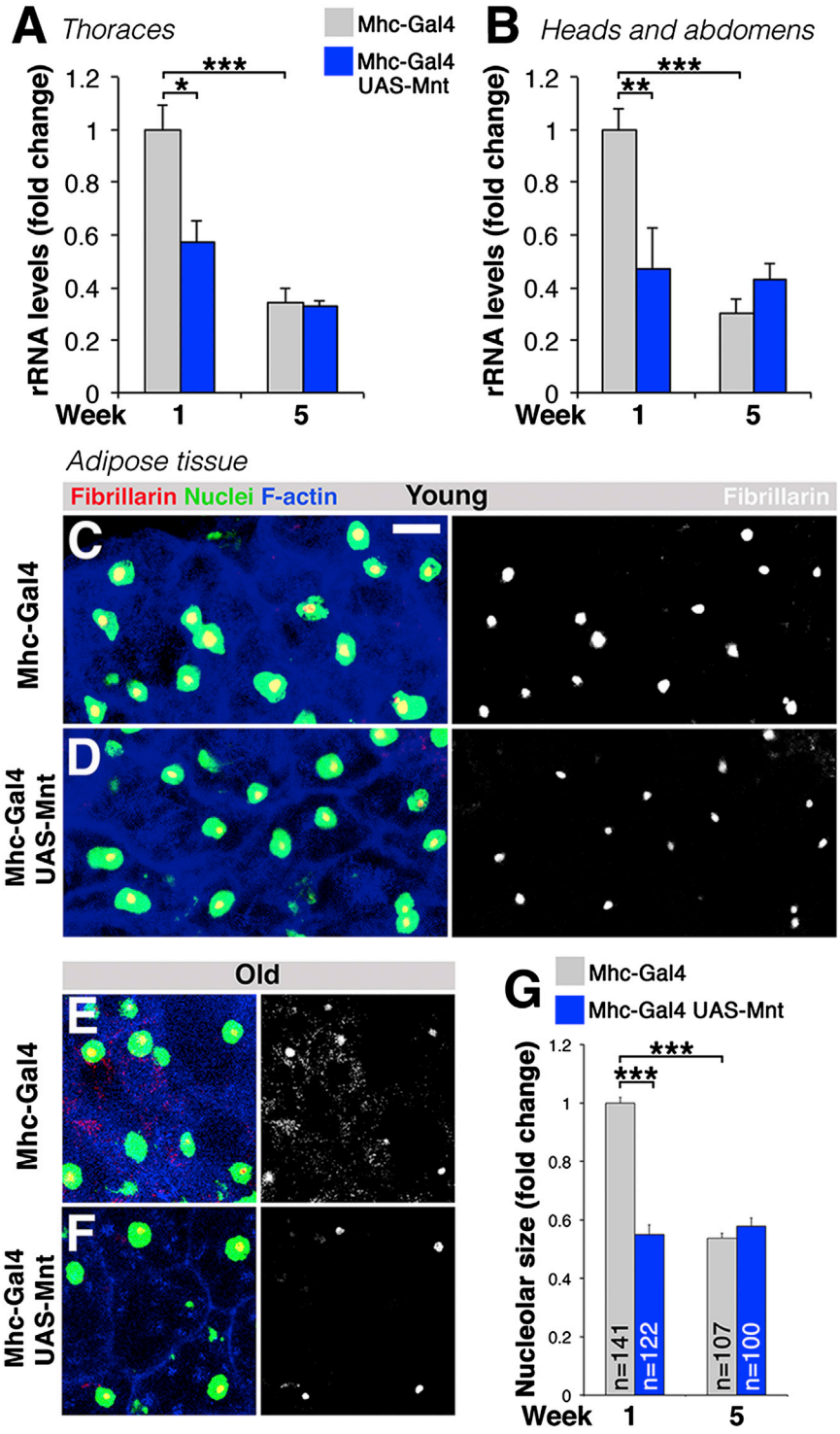

Figure 2. *Mnt* Overexpression in Muscle Systemically Regulates rRNA Levels and Nonautonomously Reduces Nucleolar Size in Adipocytes

(A and B) qRT-PCR analysis of rRNA levels in fly thoraces (which consist mostly of skeletal muscle) and heads and abdomens (which consist mostly of nonmuscle tissues) from flies overexpressing *Mnt* specifically in muscle with the *Mhc-Gal4* driver. rRNA levels decline during aging in thoraces, heads, and abdomens. Flies overexpressing *Mnt* in skeletal muscle (*Mhc-Gal4/UAS-Mnt*) display low levels of rRNA already in young age in both thoraces (A) and heads and abdomens (B) in comparison with control flies (*Mhc-Gal4/+*). SEM and n are indicated with $^{*}p < 0.05$, $^{**}p < 0.01$, and $^{***}p < 0.001$; two-way ANOVA followed by Tukey's post test.

(C–F) As compared with controls (C and E), overexpression of *Mnt* in skeletal muscle decreases the nucleolar size of adipocytes already in young age (D), anticipating the decline typically observed in old age (E and F). The nucleolar marker fibrillarin (red) is shown together with DAPI staining for nuclei (green) and F-actin (phalloidin; blue). Scale bar is 10 μm.

(G) Nucleolar size quantification is shown with SEM and n indicated; $^{*}p < 0.05$; $^{**}p < 0.01$; $^{***}p < 0.001$; two-way ANOVA followed by Tukey's post test.

See also Figure S4.

median lifespan as compared to *white* RNAi and upstream activating sequence (UAS)-RNAi alone controls (Figures 1F and 1G; Figure S3), suggesting that a partial reduction in nucleolar function can delay aging.

Mnt Activity in Skeletal Muscle Nonautonomously Decreases Nucleolar Size in Adipocytes and rRNA levels

Considering that Mnt decreases the expression of several nucleolar components (Figure 1), we next tested whether Mnt also reduces nucleolar function. By measuring ribosomal 28S rRNA levels, which are indicative of the functional status of the nucleolus, we found that *Mnt* overexpression in muscle resulted in lower 28S rRNA levels when compared to controls (Figure 2A). We also found that rRNA levels decrease during aging, indicating that Mnt prematurely induces this decline (Figure 2A).

Aging is characterized by the occurrence of degenerative changes as well as by compensatory stress responses that counteract aging itself (Haigis and Yankner, 2010). Considering that RNAi interventions mimicking decreased nucleolar function downstream of Mnt. Considering that ribosome biogenesis is the major functional output of the nucleolus (Dimario, 2004), we phenocopied decreased nucleolar function by knocking down proteins required for rRNA processing and ribosome biogenesis and function. RNAi against *CG5033*, *Nopp140*, *RpLP0*, *RpS3*, *eIF-4a*, *Brf*, and *Ssrp* in muscles extended the

extend the median lifespan (Figure S3), a reduction in rRNA levels is most likely part of a protective stress response activated during aging and induced by Mnt.

While *Mnt* overexpression in muscle led to lower rRNA levels in thoraces, which consist mostly of muscle (Figure 2A), it also induced a similar response in heads and abdomens, which are enriched in nonmuscle tissues (Figure 2B). The observation that Mnt activity solely in muscle regulates rRNA levels systemically (Figure 2B) suggests that Mnt contributes to the intertissue communication that has been proposed to be an important determinant of aging and lifespan in multiple species.

On this basis, we next asked whether the Mnt-induced systemic regulation of rRNA levels also entails cellular changes in distant tissues. Specifically, we tested whether muscle-restricted overexpression of *Mnt* regulates nucleolar size in the adipose tissue, a key target tissue for metabolic crosstalk with muscle in mammals and *Drosophila* (Demontis et al., 2013a). The size of the nucleolus is representative of its functional status and can be monitored with antibodies against the nucleolar component fibrillarin/Nop1p (Boulon et al., 2010; Dimario, 2004). Consistent with a nonautonomous role for Mnt in regulating the nucleolus, *Mnt* overexpression in skeletal muscle led to smaller nucleoli in adipocytes of young flies (Figures 2D and 2G) as compared with controls (Figure 2C).

By comparing adipocytes from young and old control flies, we also found that a decrease in nucleolar size is observed during aging (Figures 2C, 2E, and 2G), and that Mnt prematurely induces this response (Figures 2C–2G). Conversely, adipocytes from $Mnt^{-/-}$ null flies, which are short-lived (Loo et al., 2005), had larger nucleoli than controls throughout aging (Figure S4).

Altogether, these findings indicate that Mnt activity in skeletal muscle nonautonomously regulates nucleolar size in adipocytes and that the nucleolus is dynamically regulated during aging.

Transgenic RNAi Screening Identifies Myoglianin as a Myokine Regulating Lifespan and Induced by Mnt

The observation that Mnt activity in muscle nonautonomously regulates the nucleolus in adipocytes suggests a possible role of factors released by muscles and induced by Mnt. Several cytokines and growth factors, known as myokines, are known to be secreted by skeletal muscle and transduce signals from muscle to distant tissues in humans (Demontis et al., 2013a; Pedersen and Febbraio, 2012). To identify myokines regulating lifespan in *Drosophila*, we used the skeletal muscle-specific *Mhc-Gal4* driver to perform a transgenic RNAi screen with a set of *UAS-RNAi* transgenes encoding known secreted proteins (Figure 3A). No developmental or growth defects were observed under any of the RNAi treatments, consistent with the previous finding that the *Mhc-Gal4* line used drives only minimal transgene expression during skeletal muscle development (Demontis and Perrimon, 2010). To identify lifespan regulators, the survival of cohorts of male flies with a given RNAi treatment in muscle was monitored during aging and compared to a control syngenic RNAi treatment against *white* (Figure 3A). RNAi knockdowns that decreased the median lifespan included 2 independent RNAi lines against *myoglianin* (Figures 3B and S5), which also increased the percentage of flies with climbing defects in old age as compared to controls (Figures 3C and S5). Myoglianin is a secreted transforming growth factor β (TGF-β) ligand expressed primarily in glial cells and skeletal muscle in *Drosophila* (Awasaki et al., 2011; Lo and Frasch, 1999; Serpe and O'Connor, 2006) and orthologous to human Myostatin/Growth Differentiation Factor-8 (GDF8) and the related factor GDF11 (Figure 3D). In mammals, Myostatin inhibits muscle growth and regeneration (Lee, 2004; McPherron et al., 1997; Sartori et al., 2013), but neither Myostatin nor GDF11 has been implicated in lifespan determination.

Given the high degree of sequence conservation of this myokine across species and its role in lifespan determination in *Drosophila* (Figure 3), we next tested whether Myoglianin is a myokine regulated by Mnt. As indicated by qRT-PCR, *myoglianin* expression increased in skeletal muscle overexpressing *Mnt*, whereas muscle from $Mnt^{-/-}$ null flies had lower *myoglianin* mRNA levels (Figure 3E). To further confirm the role of Mnt in regulating *myoglianin* expression, we generated luciferase transcriptional reporters based on the *myoglianin* gene promoter. In agreement with in vivo findings (Figure 3E), *Mnt* overexpression in *Drosophila* S2R+ cells resulted in higher *myoglianin*-luciferase reporter activity than *yellow fluorescent protein* (*YFP*) overexpression (Figure 3F). Taken together, these results indicate that the *Drosophila* Myostatin/GDF11 ortholog Myoglianin is a myokine that is induced by Mnt.

Mnt/Myoglianin Signaling Regulates Lifespan

We next asked whether *myoglianin* overexpression regulates lifespan. Similar to *Mnt* (Figure 1), *myoglianin* overexpression in muscle extended both the median and maximum lifespan (Figure 4A) and resulted in a lower percentage of flies with climbing defects during aging (Figure 4B) as compared with isogenic controls. Lifespan extension and preservation of climbing ability was also obtained by overexpressing *myoglianin* in adulthood with dMef2-Gal4 under the temporal control of $Gal80^{ts}$ (Figure S3). Opposite to *myoglianin* overexpression, RNAi against *myoglianin* shortened the median lifespan (Figure 4C) and resulted in a higher percentage of age-related climbing defects (Figure 4D) as compared to RNAi against *white*. Notably, heterozygous UAS-transgene alone controls did not cause changes in lifespan and climbing without the *Mhc-Gal4* driver (Figures 4A–4D). In addition, no significant changes in muscle mass, body weight, and feeding behavior were observed upon *myoglianin* overexpression and RNAi with the *Mhc-Gal4* driver (Figure S2 and data not shown).

Considering that Mnt regulates *myoglianin* levels (Figure 3) and that both Mnt and Myoglianin extend lifespan (Figures 1 and 4), we next asked whether Myoglianin contributes to the lifespan extension that follows Mnt activation in muscles. To this end, a recombined line carrying the *Mhc-Gal4* and *UAS-Mnt* transgenes was crossed with RNAi lines targeting either *myoglianin* or *white* (control). A decrease in *myoglianin* mRNA levels reduced the lifespan extension and preservation of muscle function associated with *Mnt* overexpression (Figures 4E, 4F, and S6), indicating that Myoglianin contributes in part to the prolongevity effects of Mnt.

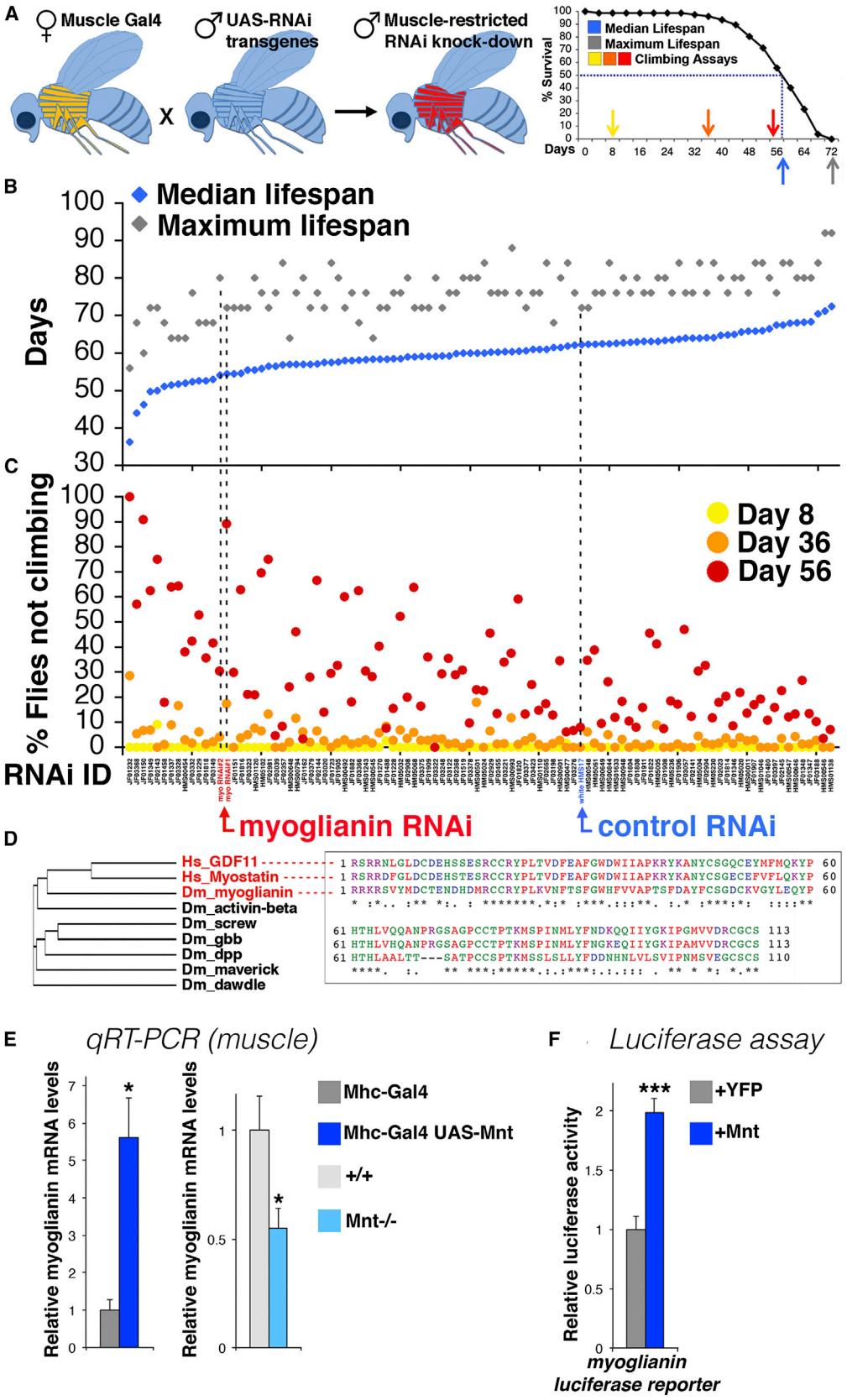

(legend on next page)

Muscle-Derived Myoglianin Regulates rRNA Levels Organism-wide

In mammals, both Myostatin and GDF11 are detected in the circulation (Souza et al., 2008; Zimmers et al., 2002), from where they have been proposed to act on nonmuscle cells (McPherron, 2010). Considering that Myoglianin acts downstream of Mnt in regulating lifespan (Figures 3 and 4), we asked whether muscle-derived Myoglianin regulates rRNA levels in muscle and nonmuscle tissues as observed following *Mnt* overexpression in muscle. In agreement with this scenario, rRNA levels decreased in young age in thoraces (Figure 5A) and heads and abdomens (Figure 5B) in response to *myoglianin* overexpression in muscle, anticipating the age-related decline in rRNA levels observed in control flies (Figures 5A and 5B).

We next asked whether *myoglianin* knockdown in muscle also elicits systemic effects. Opposite to its overexpression, *myoglianin* RNAi in muscle led to higher rRNA levels in old age in both thoraces and heads and abdomens, partially preventing the decline in rRNA levels observed during aging (Figures 5C and 5D). Taken together, these findings indicate that Myoglianin regulates rRNA levels in the whole organism during aging.

Muscle-Derived Myoglianin Regulates Nucleolar Size in Adipocytes via p38 MAPK

Given the role of Myoglianin in regulating rRNA levels, we next tested whether muscle-derived Myoglianin regulates nucleolar size in adipocytes. To this purpose, *myoglianin* was overexpressed specifically in skeletal muscle with the *Mhc-Gal4* line. As compared with controls (Figures 6A, 6B, and 6I), *myoglianin* overexpression in muscle led to smaller nucleoli in adipocytes (Figures 6C and 6D). Conversely, RNAi-mediated knockdown of *myoglianin* specifically in muscle led to increased nucleolar size in adipocytes throughout aging (Figures 6G and 6H) as compared to RNAi against *white* (Figures 6E, 6F, and 6J). Altogether, these findings indicate that Myoglianin is a myokine that regulates nucleolar size in adipocytes during aging.

Myostatin and GDF11 can signal via the activation of several intracellular effectors in mammals (Lee, 2004). We therefore sought to determine the Myoglianin signal transducers that regulate nucleolar function in this context. In response to Mnt/Myoglianin signaling, we detected substantial changes in the phosphorylation and hence activity of the stress-sensing kinase p38 MAPK (Figure 7A), a known transducer of Myostatin and TGF-β signaling in mammals (Li et al., 2008; Moustakas and Heldin, 2005; Philip et al., 2005). Interestingly, p38 MAPK protects from age-dependent motor deficits and extends lifespan in multiple species (Vrailas-Mortimer et al., 2011; Youngman et al., 2011), suggesting that it may play an important role downstream of Mnt/Myoglianin signaling. Increased phospho-p38 MAPK levels were detected in both thoracic fractions (consisting of transgene expressing muscles) and head and abdominal fractions (enriched in nonmuscle tissues with no transgene expression) from young and old flies with either *Mnt* or *myoglianin* overexpression in muscles in comparison to controls (Figure 7A). Conversely, *myoglianin* knockdown in muscles led to a decline in phospho-p38 MAPK levels in both muscle and nonmuscle tissues compared with mock RNAi treatments against *white* (Figure 7A). Similar changes in phospho-p38 MAPK levels were observed in muscle overexpressing *Mnt* and having *myoglianin* knockdown (Figure S7). There were no changes in phospho-p38 MAPK in UAS-alone controls in the absence of Gal4-driven transgene expression (Figure S7). Moreover, total p38 levels did not change in response to *Mnt* and *myoglianin* overexpression and RNAi, indicating that Mnt and Myoglianin regulate p38 activity rather than total p38 protein levels (Figure S7). In addition, no changes in phospho-p70 S6K levels were detected (Figure S7). Taken together, these findings suggest that Mnt activity in muscles and Myoglianin levels are sensed systemically via p38 MAPK phosphorylation and activation in target tissues.

To investigate whether p38 MAPK regulates nucleolar size in adipocytes, we overexpressed wild-type (WT) or dominant-negative (kinase-dead [KD]) *p38 MAPK* in adipocytes with *ppl-Gal4*. Increased levels of p38 WT led to smaller nucleoli

Figure 3. Muscle-Restricted RNAi Screening Identifies Myoglianin, a Myokine Regulating Lifespan and Induced by Mnt

(A) Scheme of the RNAi screen for myokines regulating lifespan and age-related muscle dysfunction in the fruit fly *Drosophila melanogaster*. Females carrying the *Mhc-Gal4* driver (specific for skeletal muscles) were crossed with males from a collection of Gal4-responsive *UAS-RNAi* transgenes, generated in a similar genetic background, to knock down a given cytokine or growth factor specifically in the skeletal muscle of the progeny. Climbing ability (indicative of neuromuscular function) was measured in young (day 8, yellow arrow) and older (day 36, orange arrow; and day 56, red arrow) ages, together with the median lifespan (the day at which 50% of flies are alive; blue arrow) and the maximum lifespan (the day at which the last fly in a cohort is alive; gray arrow).

(B) RNAi screen results ordered by ascending median lifespan. Each blue dot represents the median lifespan (indicated in days on the y axis) of a cohort of typically 60 flies with a muscle-specific RNAi intervention (TRiP RNAi ID is shown on the x axis of the graph in C, see also Figure S5). Corresponding gray dots represent the maximum lifespan of the same cohort. Two different RNAi treatments in skeletal muscles against the TGF-β ligand *myoglianin* (arrow and name in red) shortened the median lifespan as compared with a control RNAi against *white* (arrow and name in blue). RNAi in muscle for several Insulin-like peptides extended lifespan (Figure S5).

(C) The percentage of flies with climbing defects at day 8 (yellow), 36 (orange), and 56 (red) for the cohorts of flies with lifespan reported in (B). *Myoglianin* RNAi increased the percentage of flies with climbing defects in old age as compared with a control RNAi against *white*. Note that none of the RNAi treatments resulted in climbing defects in young age (day 8), indicating that the differences observed in older age are not due to developmental defects. See Supplemental Experimental Procedures and Figure S5 for statistical analysis of the screen.

(D) Phylogenetic analysis of *Drosophila* BMP and TGF-β ligands shows that Myoglianin is the sole *Drosophila* homolog of the highly related human TGF-β ligands Myostatin (GDF8) and GDF11. Alignment of the mature *Drosophila* Myoglianin and human GDF11 and Myostatin peptides shows extensive sequence identities (47%; *) and similarities (69%; :).

(E) *Mnt* overexpression in skeletal muscles significantly increased *myoglianin* expression, whereas muscles from $Mnt^{-/-}$ null flies had lower *myoglianin* mRNA levels. SEM is indicated with n = 4; *p < 0.05; unpaired two-tailed Student's t test.

(F) Overexpression of *Mnt* (blue) in *Drosophila* S2R+ cells resulted in higher *myoglianin*-luciferase reporter activity than controls (*YFP* overexpression; gray). SEM is indicated with n = 16; ***p < 0.001; unpaired two-tailed Student's t test.

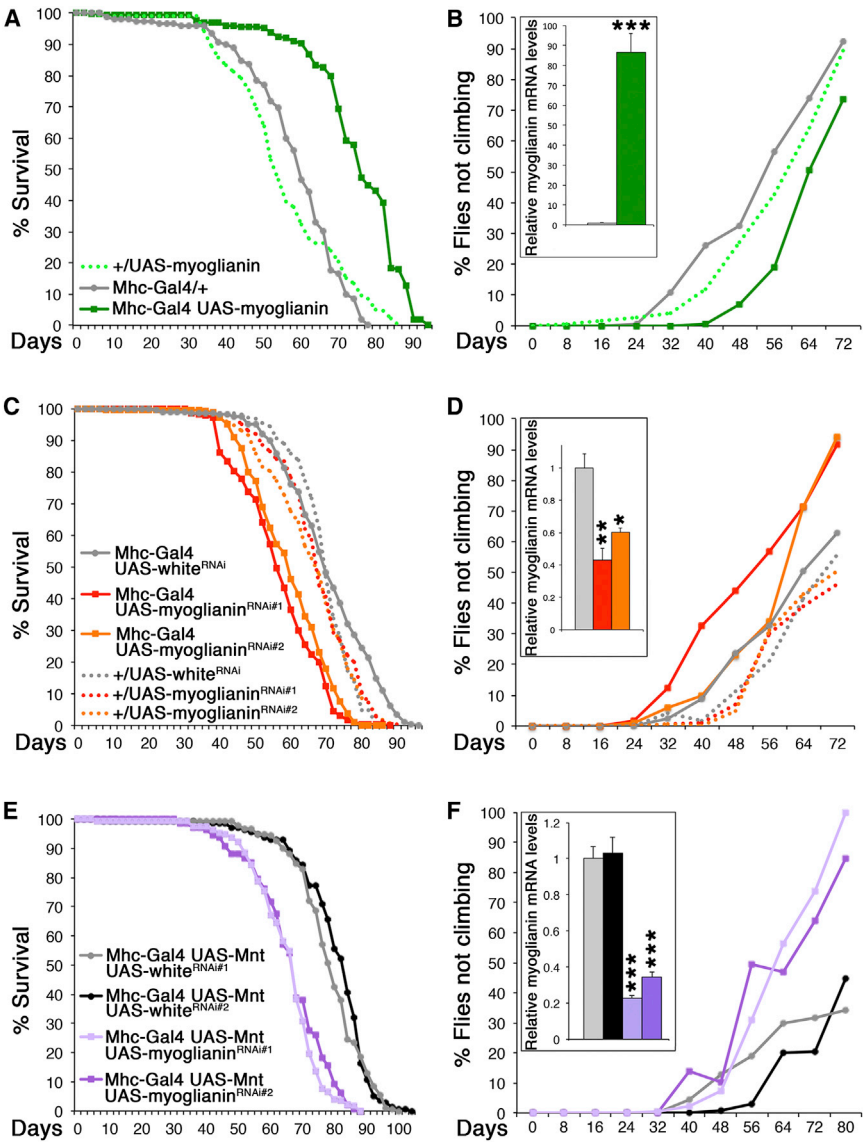

Figure 4. Mnt/Myoglianin Signaling Regulates Lifespan and Muscle Function during Aging

(A and B) *Myoglianin* overexpression (*Mhc-Gal4/UAS-myoglianin*; green; n = 458; median/maximum lifespan = 75.5/94 days) in skeletal muscles extended the median and maximum lifespan (A; $p < 0.0001$; log-rank test) and reduced the percentage of flies with age-related climbing defects (B; $p < 0.01$; log-rank test) as compared with isogenic control siblings (*MhcGal4/+*; gray; n = 152; median/maximum lifespan = 59.3/78 days) and heterozygous UAS-transgene-alone controls (*UAS-myoglianin/+*; green dotted line; n = 370; median/maximum lifespan = 53/86 days).

(C) Muscle-specific knockdown of *myoglianin* (RNAi#1: red; n = 275; median/maximum lifespan = 55.9/88 days; RNAi#2: orange; n = 731; median/maximum lifespan = 59.1/86 days) shortened the median lifespan ($p < 0.0001$; log-rank test) as compared with *white* knockdown (gray, control; n = 290; median/maximum lifespan = 69.5/96 days) and heterozygous flies carrying UAS-RNAi transgenes alone (*UAS-myoglianin$^{RNA\#1}$/+*: red dotted line, n = 367; median/maximum lifespan = 67.2/92 days; *UAS-myoglianin$^{RNAi\#2}$/+*: orange dotted line, n = 323; median/maximum lifespan = 67.1/92; and *UAS-white^{RNAi}/+*: gray dotted line, n = 307; median/maximum lifespan = 69.6/88).

(D) The percentage of flies with climbing defects progressively increased during aging in controls but to a greater extent in flies with *myoglianin* knockdown in muscles ($p < 0.01$; log-rank test).

(E) *Myoglianin* knockdown (RNAi#1: pink, n = 142; median/maximum lifespan = 66.5/88 days; and RNAi#2: violet, n = 192; median/maximum lifespan = 66.6/88 days) reduced the lifespan extension resulting from *Mnt* overexpression in muscles ($p < 0.001$; log-rank test) as compared with control *white* knockdowns (RNAi#1: gray, n = 140; median/maximum lifespan = 78.2/100 days; and RNAi#2, black, n = 179; median/maximum lifespan = 82.4/104).

(F) A higher percentage of flies with climbing defects was observed during aging when *myoglianin* levels were reduced in skeletal muscles overexpressing *Mnt* ($p < 0.01$; Log-rank test).

In all panels, relative *myoglianin* mRNA levels are shown in insets with n = 4 and SEM indicated; *$p < 0.05$, **$p < 0.01$, and ***$p < 0.001$; unpaired two-tailed Student's t test.

See also Figures S3 and S6.

(Figures 7B, 7C, and 7H) than those in controls (Figures 7D, 7E, and 7H). Conversely, *p38 KD* overexpression led to increased nucleolar size throughout aging (Figures 7F–7H), even when *myoglianin* was concomitantly overexpressed (Figure 7I), indicating that p38 MAPK activity is a key regulator of nucleolar size in adipocytes downstream of Myoglianin.

DISCUSSION

In multicellular organisms, crosstalk between tissues and organs is responsible for the homeostatic regulation of many physiological functions. Recent evidence suggests that intertissue signaling is also an important determinant of systemic aging and lifespan (Panowski and Dillin, 2009; Russell and Kahn, 2007). However, the key tissues, signaling pathways, and endocrine factors involved in this long-distance communication are only in part known. In this study, we have identified an intertissue myokine-based longevity pathway that mediates the crosstalk between skeletal muscle and adipose tissue during aging via the transcription factor Mnt and the myokine Myoglianin (Figure 7J). The activity of the transcription factor Mnt in skeletal muscles leads to both local and systemic responses that delay whole-organism aging. Cell autonomously, Mnt reduces the function of the nucleolus by decreasing the

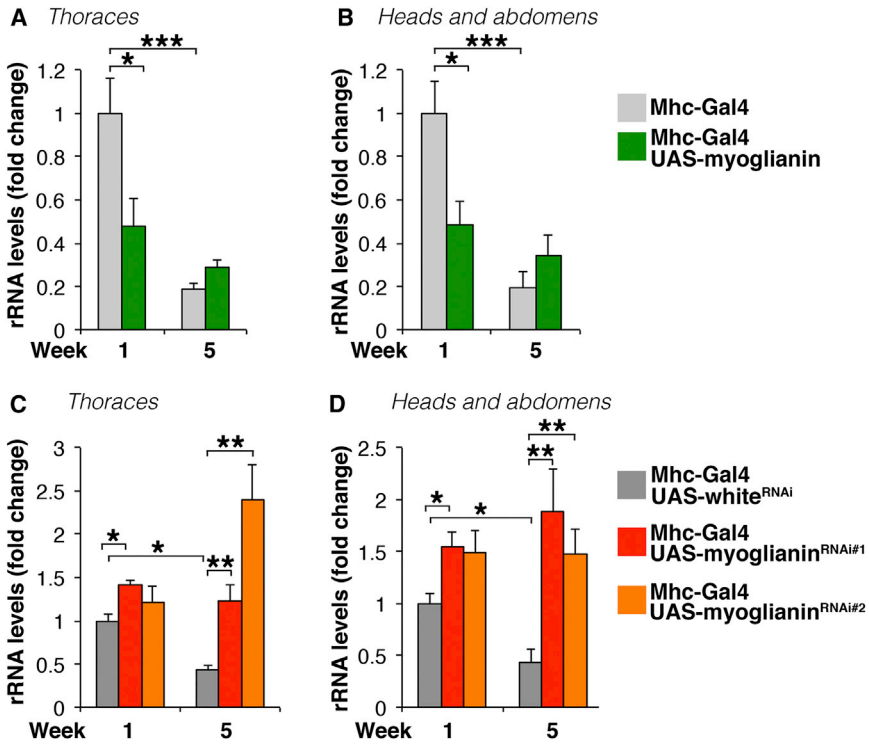

Figure 5. Muscle-Derived Myoglianin Regulates Nucleolar Function during Aging

qRT-PCR analysis of rRNA levels in fly thoraces (which consist mostly of skeletal muscle) and heads and abdomens (which consist mostly of nonmuscle tissues) from flies expressing different levels of *myoglianin* in skeletal muscle.

(A and B) rRNA levels decline during aging in thoraces, heads, and abdomens. Flies overexpressing *myoglianin* in skeletal muscle (*Mhc-Gal4/UAS-myoglianin*) display low levels of rRNA already in young age in both thoraces and heads and abdomens in comparison with control flies (*Mhc-Gal4/+*).

(C and D) rRNA levels do not decline during aging in thoraces, heads, and abdomens from flies with *myoglianinRNAi* in skeletal muscle (*Mhc-Gal4/UAS-myoglianinRNAi*) in comparison with control flies (*Mhc-Gal4/UAS-whiteRNAi*).

In all panels, n = 4 and SEM is indicated; $^{*}p < 0.05$, $^{**}p < 0.01$, and $^{***}p < 0.001$; two-way ANOVA followed by Tukey's post test.

expression of nucleolar genes and rRNA levels in muscle. In addition, Mnt increases the expression of *myoglianin* in muscle and this myokine has both local and systemic effects. In muscle, Myoglianin reduces rRNA levels and age-related muscle dysfunction. Systemically, muscle-restricted *myoglianin* overexpression leads to lower rRNA levels and reduces nucleolar size in adipocytes by modulating the activity of the stress-sensing kinase p38 MAPK. Direct binding of Myoglianin to its cellular receptor and activation of TAK1 (TGF-β-activated kinase 1) may be responsible for the regulation of p38 MAPK activity in muscle and the adipose tissue, as previously observed in mammals (Li et al., 2008; Moustakas and Heldin, 2005; Philip et al., 2005).

We fond that a prominent cellular response induced by Mnt/Myoglianin/p38 MAPK signaling is the regulation of nucleolar function. The nucleolus is a key promoter of cellular anabolism (Dimario, 2004), and its activity is reduced in response to several genetic and pharmacological interventions that are known to extend lifespan (Grewal et al., 2007; Hoppe et al., 2009; Iadevaia et al., 2012; Zhang et al., 2000). In line with the notion that a moderate reduction in cellular anabolism and protein translation delays aging (Hansen et al., 2007; Kenyon, 2010; Pan et al., 2007; Steffen et al., 2008; Syntichaki et al., 2007), we have found that decreasing nucleolar function is a protective response induced to counteract aging and sufficient to extend lifespan.

The coordinated regulation of the nucleolus across aging tissues via Myoglianin may represent an assurance mechanism to delay tissue aging systemically and to robustly extend lifespan in response to localized activity of the transcription factor Mnt in muscle. Considering that skeletal muscle constitutes the major reservoir of proteins in the organism (Wolfe, 2006) and that it has high levels of ribosome biogenesis (Drummond et al., 2009), which occurs in the nucleolus, sensing and regulating the functional status of the nucleolus in this tissue may be of particular relevance for coordinating the aging of different tissues and determining lifespan.

The Myoglianin orthologs Myostatin and GDF11 may regulate lifespan and have similar endocrine roles in humans since they are circulating factors detected in the bloodstream (Souza et al., 2008; Zimmers et al., 2002) and may act on several target tissues, including adipocytes (Feldman et al., 2006; McPherron, 2010). In agreement with this scenario, GDF11 has been recently shown to act systemically to delay heart aging in mice (Loffredo et al., 2013). Future studies in mice shall test whether GDF11 exerts this function via the modulation of p38 MAPK and the nucleolus.

In addition to systemic effects, we found that Mnt and Myoglianin have cell-autonomous/autocrine effects in preserving muscle function during aging. Specifically, overexpression of *Mnt* and *myoglianin* in muscle preserves the flies' climbing ability during aging, whereas *myoglianin* RNAi has converse effects. Considering that there are no changes in muscle mass in the adult *Drosophila* (Piccirillo et al., 2014) and in response to Mnt/Myoglianin signaling in adult flies (Figure S2), the prevention of age-related motor dysfunction by Mnt/Myoglianin signaling in this context does not entail changes in muscle mass but rather derives at least in part from the activation in preexisting myofibers of p38 MAPK, which is known to prevent age-related muscle functional decline in *Drosophila* (Vrailas-Mortimer et al., 2011). In line with these findings, Myostatin knockout mice have decreased force generation when normalized to the cross-sectional area of the muscle (specific force) and may thus experience proportionally higher myofiber functional decay during aging than control mice, although they

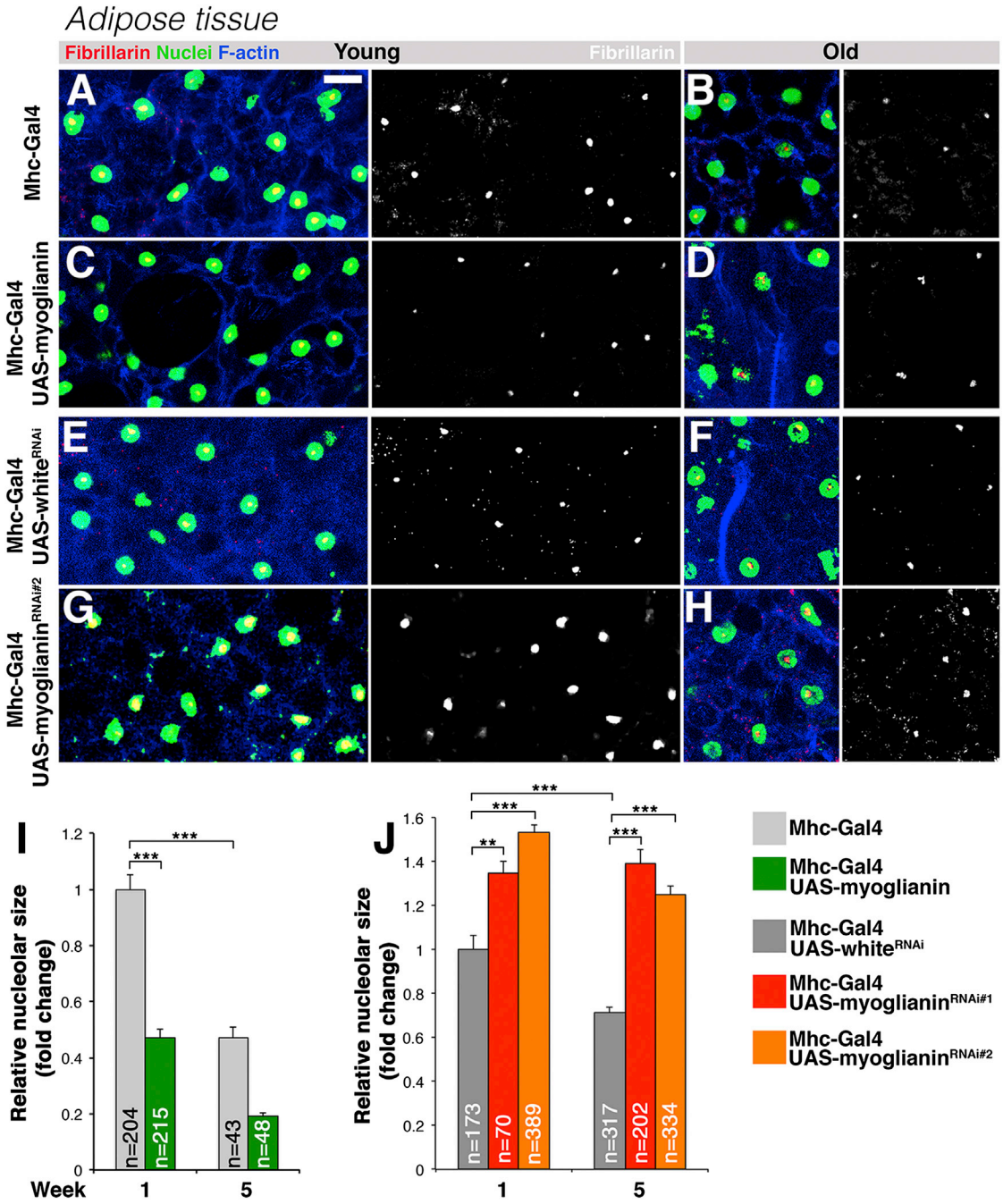

Figure 6. Muscle-Derived Myoglianin Regulates Nucleolar Size in Adipocytes

(A–H) Immunostaining of adipose tissue for the nucleolus (fibrillarin; red), F-actin (phalloidin; blue), and nuclei (DAPI; green). (C and D) Overexpression of *myoglianin* in skeletal muscles decreased the nucleolar size of adipocytes already in young age as compared with controls (A), anticipating the decline in nucleolar size typically observed in old age (B). (G and H) Muscle-restricted *myoglianin* RNAi increased nucleolar size in adipocytes in young and old age, in comparison with a control RNAi against *white* (E and F). Scale bar is 10 μm.

(I and J) Nucleolar size quantification is shown with SEM and n indicated; $^{**}p < 0.01$; $^{***}p < 0.001$; two-way ANOVA followed by Tukey's post test.

have a higher muscle mass than controls (Amthor et al., 2007; Gentry et al., 2011).

Altogether, this study highlights a key role for myokine signaling in lifespan regulation and in the integration of signaling events in different tissues during aging. Therapeutic interventions aimed at modulating myokine levels and their systemic signaling may extend healthy lifespan by simultaneously delaying age-related changes in muscle and other aging tissues.

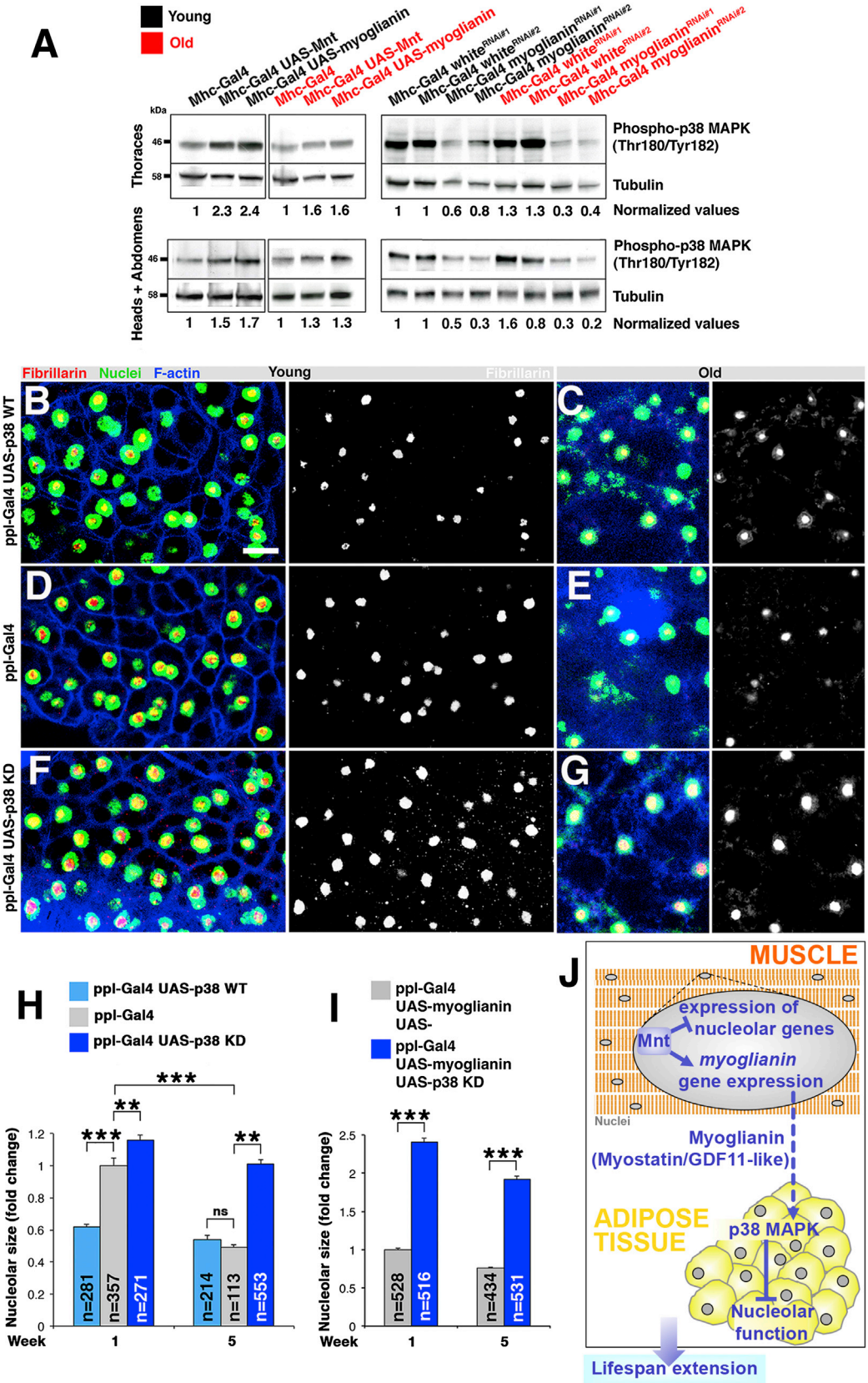

(legend on next page)

EXPERIMENTAL PROCEDURES

Lifespan Analysis

For survival analysis, male flies were collected within 24 hr from eclosion and reared at standard density (20 per vial) on cornmeal/soy flour/yeast fly food at 25°C and 60% humidity. Dead flies were counted every 2 days and the food was changed. The median lifespan was calculated by interpolation and corresponds to the day at which 50% of the flies in a cohort are alive. The maximum lifespan is the day at which the last fly in a cohort dies. To rule out any variation due to cytoplasmic background effects, all crosses were set up with female virgins from the w^{1118};*Mhc-Gal4*. To avoid any contribution of genetic background mutations to the observed lifespan phenotypes, *UAS-Mnt* and *UAS-myoglianin* transgenes were backcrossed through more than six generations against y^1w^{1118} to obtain isogenic male siblings carrying either a *UAS-* or no transgene (distinguished by eye color: *white*+ and *white*−, respectively). Male siblings carrying either a *UAS-* or no transgene and having the same genetic background were then crossed to homozygous w^{1118};*Mhc-Gal4* (*rosy*+ *white*−) females and the resulting male progenies were sorted (based on eye color) into isogenic transgene-expressing and transgene-nonexpressing cohorts before lifespan analysis. *UAS-* transgene expression obtained with Mhc-Gal4 was confirmed by qRT-PCR from fly thoraces, which consist mostly of skeletal muscle. Heterozygous *UAS-* transgene-alone controls were also analyzed to exclude that the observed phenotypes are due to differences in the genetic background. These flies were obtained by crossing *UAS-* males with female w^{1118} virgins isogenic to the w^{1118};*Mhc-Gal4* stock. All the progenies analyzed consisted of males. Transgenic RNAi lines used for the screen and for lifespan studies were generated in a y^1v^1 background (Ni et al., 2011) and were crossed with female virgins from the w^{1118} and the w^{1118};*Mhc-Gal4* isogenic stocks. RNAi against *white* was used as control to account for any aspecific effects deriving from the engagement of the RNAi machinery. RNAi-mediated knockdown in muscle was confirmed by qRT-PCR from fly thoraces. Heterozygous *UAS-RNAi* transgene-alone controls were also analyzed and obtained as described above. Note that the RNAi lines are on a genetic background that is different from the y^1w^{1118} (*yellow white*) genetic background of *UAS-Mnt* and *UAS-myoglianin* lines. All the experiments were done with males.

Climbing Assays

Negative geotaxis assays were performed as previously described (Rhodenizer et al., 2008). In brief, flies were gently tapped to the bottom of a plastic vial, and the number of flies that could climb to the top of the vial after 20 s was scored.

Whole-Mount Immunostaining

Whole-mount immunostaining of *Drosophila* adipose tissues (peripheral fat body of the abdomen) was done as described previously (Demontis and Perrimon, 2010; Hunt and Demontis, 2013).

qRT-PCR and Microarray Gene Expression Profiling

Total RNA was extracted with the TRIzol reagent (Life Technologies) from at least 15 thoraces from male flies per group, followed by cleanup with the RNeasy kit (QIAGEN) and on-column DNase digestion. Total RNA was reverse transcribed with the iScript cDNA synthesis kit (Bio-Rad). qRT-PCR was performed with the iQ SYBR Green Supermix and a CFX96 Real-Time PCR Detection System (Bio-Rad). *Alpha-Tubulin 84B* was used as a normalization reference. A primer pair for the *28S rRNA* was used to measure rRNA levels. Relative quantitation of mRNA levels was determined with the comparative C_T method. For microarray analysis, RNA integrity was assessed with an Agilent 2100 Bioanalyzer before cRNA synthesis and hybridization to Affymetrix *Drosophila* Genome 2.0 Arrays. Samples from three independent biological replicates per genotype were collected and analyzed.

Luciferase Assay

Luciferase assays were done as before (Demontis and Perrimon, 2009, 2010). See Supplemental Experimental Procedures for detailed information and a list of DNA plasmids used.

ACCESSION NUMBERS

Gene expression profiling data have been deposited in the NCBI Gene Expression Omnibus and are available under accession number GSE39877.

SUPPLEMENTAL INFORMATION

Supplemental Information includes Supplemental Experimental Procedures and seven figures and can be found with this article online at http://dx.doi.org/10.1016/j.celrep.2014.05.001.

AUTHOR CONTRIBUTIONS

F.D. conceived the project, designed and did most of the experiments, and wrote the manuscript with input from N.P. V.K.P. did the transgenic RNAi screen. W.R.S. analyzed microarray and RNAi screen data.

Figure 7. Mnt Activity in Muscle Remotely Activates p38 MAPK via Myoglianin to Regulate Nucleolar Size in Adipocytes

(A) Western blot analysis of fractions from either thoraces (consisting mainly of muscles; upper panels) or heads and abdomens (consisting mainly of nonmuscle tissues; lower panels) from controls and flies overexpressing *Mnt* and *myoglianin* (left panels) or with RNAi-mediated knockdown of *myoglianin* or *white* (right) in skeletal muscles from young (1 week) and old (8 weeks) flies. Mnt and Myoglianin increase the levels of active phospho-p38 MAPK in both muscle and nonmuscle tissues as compared with controls (left), whereas *myoglianin* knockdown had converse effects (right). Relative quantification of phospho-p38 MAPK levels normalized to α-tubulin is indicated. See also Figure S7.

(B–H) Adipocytes labeled with the nucleolar marker fibrillarin (red), phalloidin (F-actin; blue), and DAPI (nuclei; green). (B) In young age (1 week), wild-type (WT) *p38 MAPK* overexpression in adipocytes with the *ppl-Gal4* driver led to significantly smaller nucleoli than in controls (D and H), leading to a premature decline in nucleolar size which is otherwise normally observed in old age (C, E, and H). Conversely, bigger nucleoli were observed in young (F) and old age (G and H) after overexpression of dominant-negative, kinase-dead (KD) *p38 MAPK*.

(I) Similar results were obtained also when *myoglianin* was concomitantly overexpressed with p38 KD (*ppl-Gal4/UAS-p38KD;UAS-myoglianin/+;*), in comparison with overexpression of a *UAS-myoglianin* transgene together with an empty *UAS-* that drives no transgene expression and which is used to control for Gal4 titration effects in the different genotypes analyzed (*ppl-Gal4/UAS-; UAS-myoglianin/+;*). Scale bar is 10 μm.

Statistical analysis was done with two-way ANOVA followed by Tukey's post test in (H) and (I). In (H) and (I), n is indicated with SEM. $^{**}p < 0.01$; $^{***}p < 0.001$; ns, not significant.

(J) Summary scheme. Muscle-specific overexpression of *Mnt* extends lifespan and prevents age-related muscle functional decay. In the nuclei (gray) of myofibers (orange), the transcription factor Mnt reduces rRNA levels and the expression of components of the nucleolus, a regulator of aging. In addition, Mnt increases the expression of the TGF-β ligand *myoglianin*, the *Drosophila* ortholog of human Myostatin and GDF11. In turn, muscle-specific overexpression of *myoglianin* extends lifespan and reduces rRNA levels in the whole organism and nucleolar size in adipocytes (yellow) by activating p38 MAPK, a known transducer of TGF-β signaling, while *myoglianin* RNAi in muscle has converse effects. In addition to inducing systemic effects, Myoglianin acts in an autocrine manner to reduce rRNA levels in muscle and preserves muscle function during aging. These findings highlight that signaling events in skeletal muscle can influence systemic aging and lifespan via muscle-derived secreted proteins, i.e., myokines. Myokine-based coordination of nucleolar function across aging tissues may represent an assurance mechanism for robust lifespan determination in aging organisms.

ACKNOWLEDGMENTS

We thank the DRSC/TRiP, the Bloomington Stock Center, R. Eisenman, T. Awasaki, T. Lee, A. Vrailas-Mortimer, S. Sanyal, and P. Gallant for providing fly stocks and reagents. We are grateful to the DFCI Microarray Core, C. Villalta for embryo injection, R. Binari, and D. Rao for technical help. This work was supported by ALSAC, an Ellison Medical Foundation New Scholar in Aging award (to F.D.), and the NIH and HHMI (to N.P.).

Received: February 3, 2014
Revised: April 8, 2014
Accepted: May 1, 2014
Published: May 29, 2014

REFERENCES

Amthor, H., Macharia, R., Navarrete, R., Schuelke, M., Brown, S.C., Otto, A., Voit, T., Muntoni, F., Vrbóva, G., Partridge, T., et al. (2007). Lack of myostatin results in excessive muscle growth but impaired force generation. Proc. Natl. Acad. Sci. USA *104*, 1835–1840.

Awasaki, T., Huang, Y., O'Connor, M.B., and Lee, T. (2011). Glia instruct developmental neuronal remodeling through TGF-β signaling. Nat. Neurosci. *14*, 821–823.

Bai, H., Kang, P., Hernandez, A.M., and Tatar, M. (2013). Activin signaling targeted by insulin/dFOXO regulates aging and muscle proteostasis in Drosophila. PLoS Genet. *9*, e1003941.

Boström, P., Wu, J., Jedrychowski, M.P., Korde, A., Ye, L., Lo, J.C., Rasbach, K.A., Boström, E.A., Choi, J.H., Long, J.Z., et al. (2012). A PGC1-α-dependent myokine that drives brown-fat-like development of white fat and thermogenesis. Nature *481*, 463–468.

Boulon, S., Westman, B.J., Hutten, S., Boisvert, F.M., and Lamond, A.I. (2010). The nucleolus under stress. Mol. Cell *40*, 216–227.

Demontis, F., and Perrimon, N. (2009). Integration of Insulin receptor/Foxo signaling and dMyc activity during muscle growth regulates body size in Drosophila. Development *136*, 983–993.

Demontis, F., and Perrimon, N. (2010). FOXO/4E-BP signaling in Drosophila muscles regulates organism-wide proteostasis during aging. Cell *143*, 813–825.

Demontis, F., Piccirillo, R., Goldberg, A.L., and Perrimon, N. (2013a). The influence of skeletal muscle on systemic aging and lifespan. Aging Cell *12*, 943–949.

Demontis, F., Piccirillo, R., Goldberg, A.L., and Perrimon, N. (2013b). Mechanisms of skeletal muscle aging: insights from Drosophila and mammalian models. Dis. Model. Mech. *6*, 1339–1352.

Dimario, P.J. (2004). Cell and molecular biology of nucleolar assembly and disassembly. Int. Rev. Cytol. *239*, 99–178.

Drummond, M.J., Dreyer, H.C., Fry, C.S., Glynn, E.L., and Rasmussen, B.B. (2009). Nutritional and contractile regulation of human skeletal muscle protein synthesis and mTORC1 signaling. J. Appl. Physiol. *106*, 1374–1384.

Durieux, J., Wolff, S., and Dillin, A. (2011). The cell-non-autonomous nature of electron transport chain-mediated longevity. Cell *144*, 79–91.

Duteil, D., Chambon, C., Ali, F., Malivindi, R., Zoll, J., Kato, S., Geny, B., Chambon, P., and Metzger, D. (2010). The transcriptional coregulators TIF2 and SRC-1 regulate energy homeostasis by modulating mitochondrial respiration in skeletal muscles. Cell Metab. *12*, 496–508.

Feldman, B.J., Streeper, R.S., Farese, R.V., Jr., and Yamamoto, K.R. (2006). Myostatin modulates adipogenesis to generate adipocytes with favorable metabolic effects. Proc. Natl. Acad. Sci. USA *103*, 15675–15680.

Gates, A.C., Bernal-Mizrachi, C., Chinault, S.L., Feng, C., Schneider, J.G., Coleman, T., Malone, J.P., Townsend, R.R., Chakravarthy, M.V., and Semenkovich, C.F. (2007). Respiratory uncoupling in skeletal muscle delays death and diminishes age-related disease. Cell Metab. *6*, 497–505.

Gentry, B.A., Ferreira, J.A., Phillips, C.L., and Brown, M. (2011). Hindlimb skeletal muscle function in myostatin-deficient mice. Muscle Nerve *43*, 49–57.

Giannakou, M.E., Goss, M., Jünger, M.A., Hafen, E., Leevers, S.J., and Partridge, L. (2004). Long-lived Drosophila with overexpressed dFOXO in adult fat body. Science *305*, 361.

Grewal, S.S., Evans, J.R., and Edgar, B.A. (2007). Drosophila TIF-IA is required for ribosome synthesis and cell growth and is regulated by the TOR pathway. J. Cell Biol. *179*, 1105–1113.

Guarente, L. (1997). Link between aging and the nucleolus. Genes Dev. *11*, 2449–2455.

Haigis, M.C., and Yankner, B.A. (2010). The aging stress response. Mol. Cell *40*, 333–344.

Hakimi, P., Yang, J., Casadesus, G., Massillon, D., Tolentino-Silva, F., Nye, C.K., Cabrera, M.E., Hagen, D.R., Utter, C.B., Baghdy, Y., et al. (2007). Overexpression of the cytosolic form of phosphoenolpyruvate carboxykinase (GTP) in skeletal muscle repatterns energy metabolism in the mouse. J. Biol. Chem. *282*, 32844–32855.

Hansen, M., Taubert, S., Crawford, D., Libina, N., Lee, S.J., and Kenyon, C. (2007). Lifespan extension by conditions that inhibit translation in Caenorhabditis elegans. Aging Cell *6*, 95–110.

Hoppe, S., Bierhoff, H., Cado, I., Weber, A., Tiebe, M., Grummt, I., and Voit, R. (2009). AMP-activated protein kinase adapts rRNA synthesis to cellular energy supply. Proc. Natl. Acad. Sci. USA *106*, 17781–17786.

Hunt, L.C., and Demontis, F. (2013). Whole-mount immunostaining of Drosophila skeletal muscle. Nat. Protoc. *8*, 2496–2501.

Hurlin, P.J., and Huang, J. (2006). The MAX-interacting transcription factor network. Semin. Cancer Biol. *16*, 265–274.

Hwangbo, D.S., Gershman, B., Tu, M.P., Palmer, M., and Tatar, M. (2004). Drosophila dFOXO controls lifespan and regulates insulin signalling in brain and fat body. Nature *429*, 562–566.

Iadevaia, V., Zhang, Z., Jan, E., and Proud, C.G. (2012). mTOR signaling regulates the processing of pre-rRNA in human cells. Nucleic Acids Res. *40*, 2527–2539.

Karpac, J., Younger, A., and Jasper, H. (2011). Dynamic coordination of innate immune signaling and insulin signaling regulates systemic responses to localized DNA damage. Dev. Cell *20*, 841–854.

Katewa, S.D., Demontis, F., Kolipinski, M., Hubbard, A., Gill, M.S., Perrimon, N., Melov, S., and Kapahi, P. (2012). Intramyocellular fatty-acid metabolism plays a critical role in mediating responses to dietary restriction in Drosophila melanogaster. Cell Metab. *16*, 97–103.

Kenyon, C.J. (2010). The genetics of ageing. Nature *464*, 504–512.

Lee, S.J. (2004). Regulation of muscle mass by myostatin. Annu. Rev. Cell Dev. Biol. *20*, 61–86.

Li, Z.B., Kollias, H.D., and Wagner, K.R. (2008). Myostatin directly regulates skeletal muscle fibrosis. J. Biol. Chem. *283*, 19371–19378.

Libina, N., Berman, J.R., and Kenyon, C. (2003). Tissue-specific activities of C. elegans DAF-16 in the regulation of lifespan. Cell *115*, 489–502.

Lo, P.C., and Frasch, M. (1999). Sequence and expression of myoglianin, a novel Drosophila gene of the TGF-beta superfamily. Mech. Dev. *86*, 171–175.

Loffredo, F.S., Steinhauser, M.L., Jay, S.M., Gannon, J., Pancoast, J.R., Yalamanchi, P., Sinha, M., Dall'Osso, C., Khong, D., Shadrach, J.L., et al. (2013). Growth differentiation factor 11 is a circulating factor that reverses age-related cardiac hypertrophy. Cell *153*, 828–839.

Loo, L.W., Secombe, J., Little, J.T., Carlos, L.S., Yost, C., Cheng, P.F., Flynn, E.M., Edgar, B.A., and Eisenman, R.N. (2005). The transcriptional repressor dMnt is a regulator of growth in Drosophila melanogaster. Mol. Cell. Biol. *25*, 7078–7091.

Mayer, C., Bierhoff, H., and Grummt, I. (2005). The nucleolus as a stress sensor: JNK2 inactivates the transcription factor TIF-IA and down-regulates rRNA synthesis. Genes Dev. *19*, 933–941.

McPherron, A.C. (2010). Metabolic Functions of Myostatin and Gdf11. Immunol. Endocr. Metab. Agents Med. Chem. *10*, 217–231.

McPherron, A.C., Lawler, A.M., and Lee, S.J. (1997). Regulation of skeletal muscle mass in mice by a new TGF-beta superfamily member. Nature *387*, 83–90.

Metter, E.J., Talbot, L.A., Schrager, M., and Conwit, R. (2002). Skeletal muscle strength as a predictor of all-cause mortality in healthy men. J. Gerontol. A Biol. Sci. Med. Sci. *57*, B359–B365.

Michel, C.I., Holley, C.L., Scruggs, B.S., Sidhu, R., Brookheart, R.T., Listenberger, L.L., Behlke, M.A., Ory, D.S., and Schaffer, J.E. (2011). Small nucleolar RNAs U32a, U33, and U35a are critical mediators of metabolic stress. Cell Metab. *14*, 33–44.

Moustakas, A., and Heldin, C.H. (2005). Non-Smad TGF-beta signals. J. Cell Sci. *118*, 3573–3584.

Nair, K.S. (2005). Aging muscle. Am. J. Clin. Nutr. *81*, 953–963.

Ni, J.Q., Zhou, R., Czech, B., Liu, L.P., Holderbaum, L., Yang-Zhou, D., Shim, H.S., Tao, R., Handler, D., Karpowicz, P., et al. (2011). A genome-scale shRNA resource for transgenic RNAi in Drosophila. Nat. Methods *8*, 405–407.

Orian, A., Grewal, S.S., Knoepfler, P.S., Edgar, B.A., Parkhurst, S.M., and Eisenman, R.N. (2005). Genomic binding and transcriptional regulation by the Drosophila Myc and Mnt transcription factors. Cold Spring Harb. Symp. Quant. Biol. *70*, 299–307.

Owusu-Ansah, E., Song, W., and Perrimon, N. (2013). Muscle mitohormesis promotes longevity via systemic repression of insulin signaling. Cell *155*, 699–712.

Pan, K.Z., Palter, J.E., Rogers, A.N., Olsen, A., Chen, D., Lithgow, G.J., and Kapahi, P. (2007). Inhibition of mRNA translation extends lifespan in Caenorhabditis elegans. Aging Cell *6*, 111–119.

Panowski, S.H., and Dillin, A. (2009). Signals of youth: endocrine regulation of aging in Caenorhabditis elegans. Trends Endocrinol. Metab. *20*, 259–264.

Pedersen, B.K., and Febbraio, M.A. (2012). Muscles, exercise and obesity: skeletal muscle as a secretory organ. Nat. Rev. Endocrinol. *8*, 457–465.

Philip, B., Lu, Z., and Gao, Y. (2005). Regulation of GDF-8 signaling by the p38 MAPK. Cell. Signal. *17*, 365–375.

Piccirillo, R., Demontis, F., Perrimon, N., and Goldberg, A.L. (2014). Mechanisms of muscle growth and atrophy in mammals and Drosophila. Dev. Dyn. *243*, 201–215.

Pospisilik, J.A., Knauf, C., Joza, N., Benit, P., Orthofer, M., Cani, P.D., Ebersberger, I., Nakashima, T., Sarao, R., Neely, G., et al. (2007). Targeted deletion of AIF decreases mitochondrial oxidative phosphorylation and protects from obesity and diabetes. Cell *131*, 476–491.

Rera, M., Bahadorani, S., Cho, J., Koehler, C.L., Ulgherait, M., Hur, J.H., Ansari, W.S., Lo, T., Jr., Jones, D.L., and Walker, D.W. (2011). Modulation of longevity and tissue homeostasis by the Drosophila PGC-1 homolog. Cell Metab. *14*, 623–634.

Rhodenizer, D., Martin, I., Bhandari, P., Pletcher, S.D., and Grotewiel, M. (2008). Genetic and environmental factors impact age-related impairment of negative geotaxis in Drosophila by altering age-dependent climbing speed. Exp. Gerontol. *43*, 739–748.

Ruiz, J.R., Sui, X., Lobelo, F., Morrow, J.R., Jr., Jackson, A.W., Sjöström, M., and Blair, S.N. (2008). Association between muscular strength and mortality in men: prospective cohort study. BMJ *337*, a439.

Russell, S.J., and Kahn, C.R. (2007). Endocrine regulation of ageing. Nat. Rev. Mol. Cell Biol. *8*, 681–691.

Sartori, R., Schirwis, E., Blaauw, B., Bortolanza, S., Zhao, J., Enzo, E., Stantzou, A., Mouisel, E., Toniolo, L., Ferry, A., et al. (2013). BMP signaling controls muscle mass. Nat. Genet. *45*, 1309–1318.

Satoh, A., Brace, C.S., Rensing, N., Cliften, P., Wozniak, D.F., Herzog, E.D., Yamada, K.A., and Imai, S. (2013). Sirt1 extends life span and delays aging in mice through the regulation of Nk2 homeobox 1 in the DMH and LH. Cell Metab. *18*, 416–430.

Schuster, C.M., Davis, G.W., Fetter, R.D., and Goodman, C.S. (1996). Genetic dissection of structural and functional components of synaptic plasticity. I. Fasciclin II controls synaptic stabilization and growth. Neuron *17*, 641–654.

Serpe, M., and O'Connor, M.B. (2006). The metalloprotease tolloid-related and its TGF-beta-like substrate Dawdle regulate Drosophila motoneuron axon guidance. Development *133*, 4969–4979.

Souza, T.A., Chen, X., Guo, Y., Sava, P., Zhang, J., Hill, J.J., Yaworsky, P.J., and Qiu, Y. (2008). Proteomic identification and functional validation of activins and bone morphogenetic protein 11 as candidate novel muscle mass regulators. Mol. Endocrinol. *22*, 2689–2702.

Steffen, K.K., MacKay, V.L., Kerr, E.O., Tsuchiya, M., Hu, D., Fox, L.A., Dang, N., Johnston, E.D., Oakes, J.A., Tchao, B.N., et al. (2008). Yeast life span extension by depletion of 60s ribosomal subunits is mediated by Gcn4. Cell *133*, 292–302.

Swindell, W.R., Ensrud, K.E., Cawthon, P.M., Cauley, J.A., Cummings, S.R., and Miller, R.A.; Study Of Osteoporotic Fractures Research Group (2010). Indicators of "healthy aging" in older women (65-69 years of age). A data-mining approach based on prediction of long-term survival. BMC Geriatr. *10*, 55.

Syntichaki, P., Troulinaki, K., and Tavernarakis, N. (2007). Protein synthesis is a novel determinant of aging in Caenorhabditis elegans. Ann. N Y Acad. Sci. *1119*, 289–295.

Taguchi, A., Wartschow, L.M., and White, M.F. (2007). Brain IRS2 signaling coordinates life span and nutrient homeostasis. Science *317*, 369–372.

van Oosten-Hawle, P., Porter, R.S., and Morimoto, R.I. (2013). Regulation of organismal proteostasis by transcellular chaperone signaling. Cell *153*, 1366–1378.

Vrailas-Mortimer, A., del Rivero, T., Mukherjee, S., Nag, S., Gaitanidis, A., Kadas, D., Consoulas, C., Duttaroy, A., and Sanyal, S. (2011). A muscle-specific p38 MAPK/Mef2/MnSOD pathway regulates stress, motor function, and life span in Drosophila. Dev. Cell *21*, 783–795.

Wang, M.C., Bohmann, D., and Jasper, H. (2005). JNK extends life span and limits growth by antagonizing cellular and organism-wide responses to insulin signaling. Cell *121*, 115–125.

Wang, M.C., O'Rourke, E.J., and Ruvkun, G. (2008). Fat metabolism links germline stem cells and longevity in C. elegans. Science *322*, 957–960.

Wessells, R.J., Fitzgerald, E., Cypser, J.R., Tatar, M., and Bodmer, R. (2004). Insulin regulation of heart function in aging fruit flies. Nat. Genet. *36*, 1275–1281.

Wolfe, R.R. (2006). The underappreciated role of muscle in health and disease. Am. J. Clin. Nutr. *84*, 475–482.

Youngman, M.J., Rogers, Z.N., and Kim, D.H. (2011). A decline in p38 MAPK signaling underlies immunosenescence in Caenorhabditis elegans. PLoS Genet. *7*, e1002082.

Zhang, H., Stallock, J.P., Ng, J.C., Reinhard, C., and Neufeld, T.P. (2000). Regulation of cellular growth by the Drosophila target of rapamycin dTOR. Genes Dev. *14*, 2712–2724.

Zimmers, T.A., Davies, M.V., Koniaris, L.G., Haynes, P., Esquela, A.F., Tomkinson, K.N., McPherron, A.C., Wolfman, N.M., and Lee, S.J. (2002). Induction of cachexia in mice by systemically administered myostatin. Science *296*, 1486–1488.

Cell Reports, Volume *7*

Supplemental Information

Intertissue Control of the Nucleolus via a Myokine-Dependent Longevity Pathway

Fabio Demontis, Vishal K. Patel, William R. Swindell, and Norbert Perrimon,

SUPPLEMENTAL FIGURES AND LEGENDS

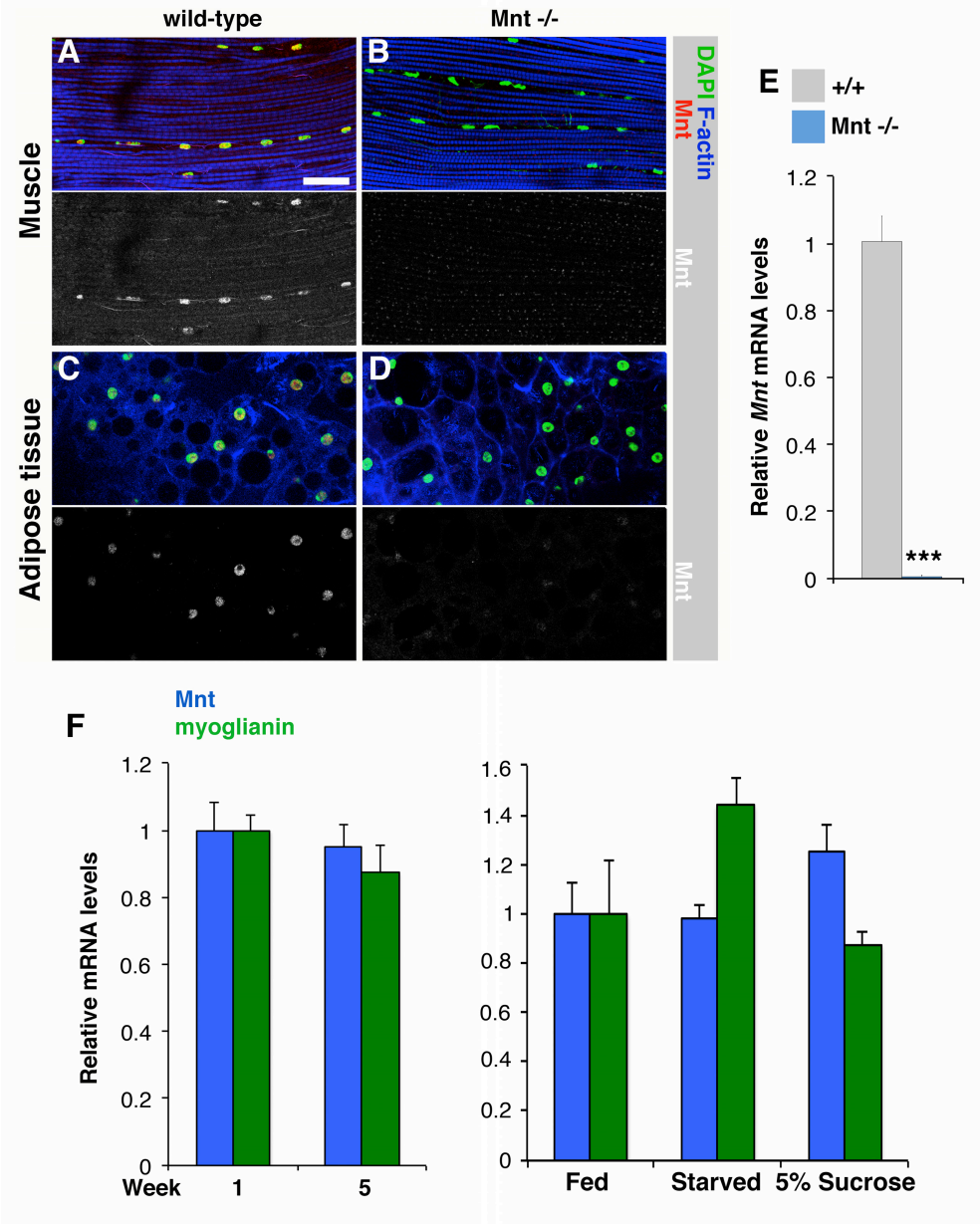

Figure S1. *Drosophila* Mnt is Detected in Skeletal Muscle and Adipose Tissue, Related to Figure 1. (A-D) Immunostaining of indirect flight muscle with anti-Mnt antibodies (red), F-actin (phalloidin, blue), and nuclei (DAPI, green). Mnt is detected in nuclei of adult skeletal muscle (A) and adipose tissue (C) from wild-type flies but not from *Mnt-/-* null flies (B, D, E). Scale bar is 20 μm. In (E), relative *Mnt* mRNA levels are shown with SEM indicated and n=4. ***P<0.001, unpaired two-tailed Student's *t*-test. (F) No apparent changes in *Mnt* and *myoglianin* mRNA levels are detected in muscle during aging and in response to starvation and a 5% sucrose diet. Mnt activity and Myoglianin signaling may be modulated via post-transcriptional mechanisms during aging independently from gene expression.

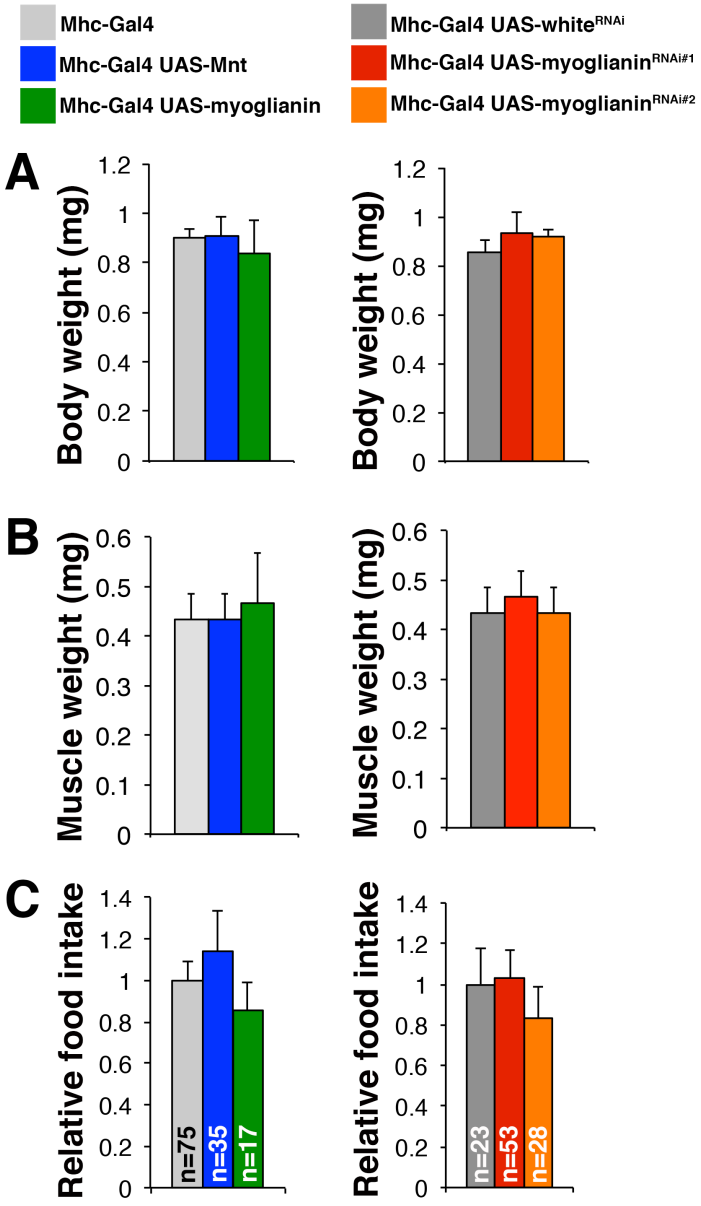

Figure S2. No Differences in Body Weight, Muscle Mass, and Relative Food Intake in Response to Mnt/Myoglianin Levels, Related to Figure 1 and 4. (A) Average body weight and (B) thoracic weight (consisting mostly of skeletal muscle and hence indicative of muscle mass) of flies overexpressing *Mnt* (blue) or *myoglianin* (green), and with *myoglianin*$^{RNAi\#1}$ and *myoglianin*$^{RNAi\#2}$ (red and orange) in muscle in comparison with controls (grey). SEM is indicated and n(batches of 10 flies)=3. No significant changes were detected by two-way ANOVA and Tukey's post test. (C) Relative food intake estimated with the capillary feeding (CAFÉ) assay reveals no substantial differences in the food intake of the genotypes analyzed. SEM and n(measurements) are indicated.

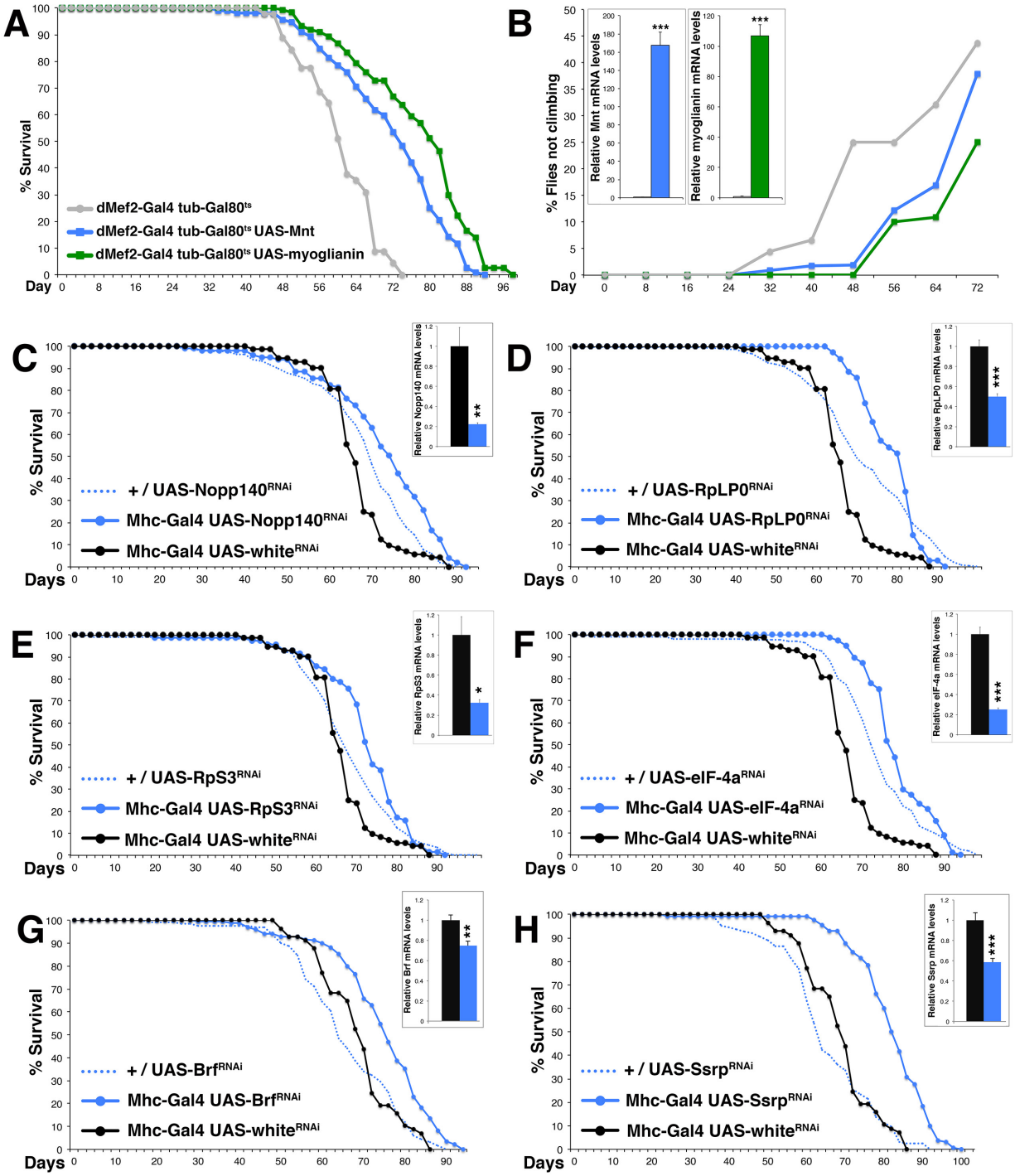

Figure S3. Lifespan Extension in Response to Mnt/Myoglianin Overexpression and RNAi-mediated knockdown of Genes Involved in Ribosome Biogenesis and Function, Related to Figure 1 and 4.

(A-B) Overexpression of *Mnt* and *myoglianin* in adult skeletal muscle with the *dMef2-Gal4* driver under the temporal control of Gal80^{ts}. Flies were raised at 18°C to avoid transgene expression during development and shifted to 25°C three days after eclosion to inactivate Gal80^{ts} and induce *Mnt* and *myoglianin*

expression in muscle of adult flies. Overexpression of *Mnt* (blue; *dMef2-Gal4/UAS-Mnt;* n=112; median/maximum lifespan=73.3/92 days) and *myoglianin* (green; *dMef2-Gal4/UAS-myoglianin;* n=121; median/maximum lifespan=80.5/98 days) in adult skeletal muscle extends lifespan (P<0.001; Log-rank tests) and decreases age-related climbing defects (P<0.01; Log-rank tests) in comparison to control flies (grey; *dMef2-Gal4/+;* n=45; median/maximum lifespan=60.2/74 days). Relative mRNA levels of *Mnt* and *myoglianin* are shown with SEM indicated and n=4. ***P<0.001, unpaired two-tailed Student's *t*-test.

(C-H) RNAi-mediated knockdown (blue) in muscle of *Nopp140* (C; n=97; median/maximum lifespan=74.1/92 days), *RpLP0* (D; n=35; median/maximum lifespan=80.2/92 days), *RpS3* (E; n=70; median/maximum lifespan=72.3/92 days), *eIF-4a* (F; n=77; median/maximum lifespan=76.5/94 days), *Brf* (G; n=170; median/maximum lifespan=75.2/94 days), and *Ssrp* (H; n=130; median/maximum lifespan=82/100) extends the median lifespan in comparison with UAS-RNAi alone controls (dashed blue line; respectively in C to H: n=166; n=271; n=396; n=271; n=132; n=125; having respectively median/maximum lifespan: 69.3/90; 69.8/100; 66.8/100; 72/98; 63.8/90; 62.6/92 days) and *white* RNAi (black; n=72 and median/maximum lifespan=65.3/88 days in C-F; n=57 and median/maximum lifespan=68.6/86 days in G-H; P<0.001; Log-rank tests).

Relative mRNA levels of *Nopp140*, *RpLP0*, *RpS3*, *eIF-4a*, *Brf*, and *Ssrp* are respectively shown in boxes in C-H**,** with SEM indicated and n=4. *P<0.05; **P<0.01; ***P<0.001, unpaired two-tailed Student's *t*-test.

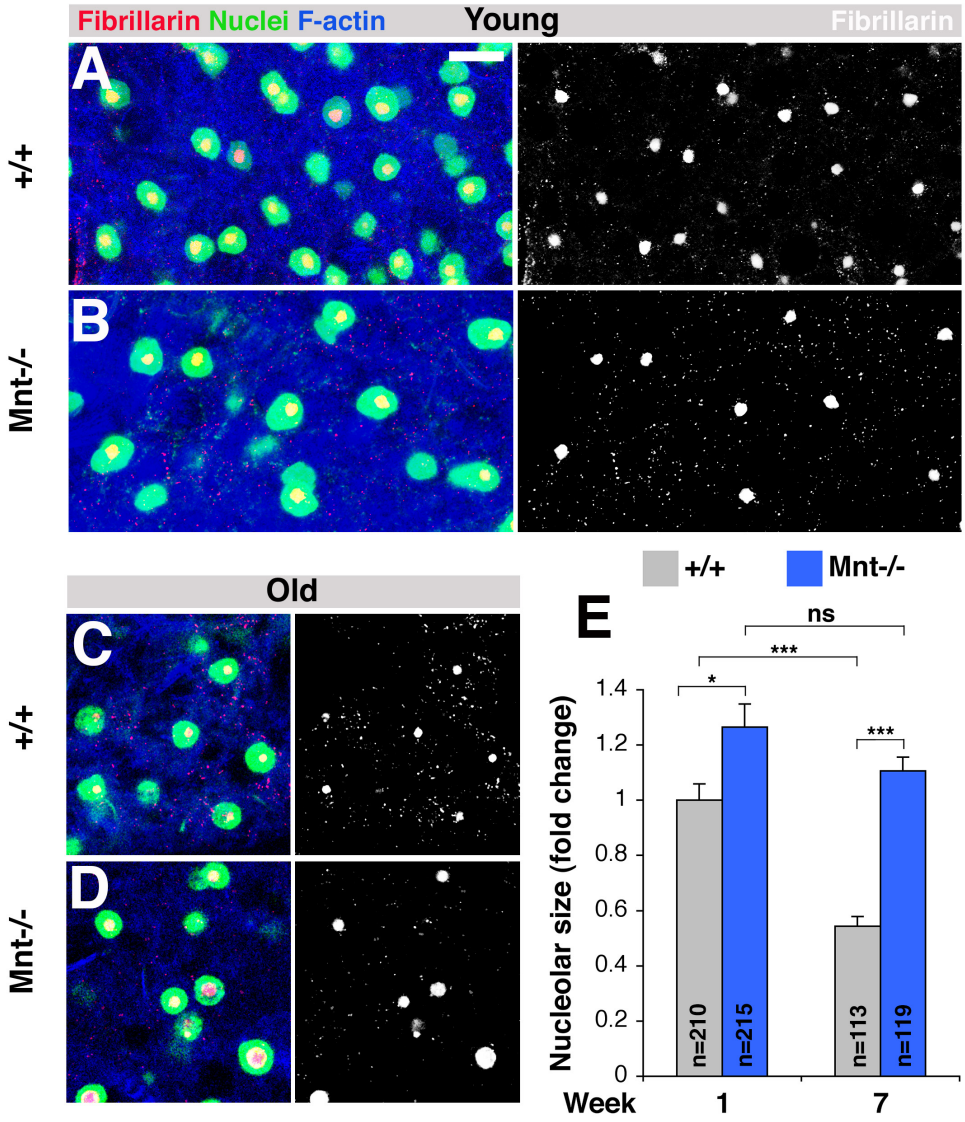

Figure S4. Regulation of Nucleolar Size in *Mnt* Null Adipocytes during Aging, Related to Figure 2. Immunostaining of adipose tissues (fat body) from control (+/+) and *Mnt*$^{-/-}$ null flies in young (1 week) and old age (7 weeks). Although nucleolar size decreases during aging in wild-type adipocytes (A-C), it does not in the absence of *Mnt* (B-D; *Mnt*$^{-/-}$). In A-D, scale bar is 10 μm. Nucleolar size quantification is shown in (E) with SEM and n indicated; ns, not significant; **P*<0.05; ****P*<0.001; two-way ANOVA followed by Tukey's post test.

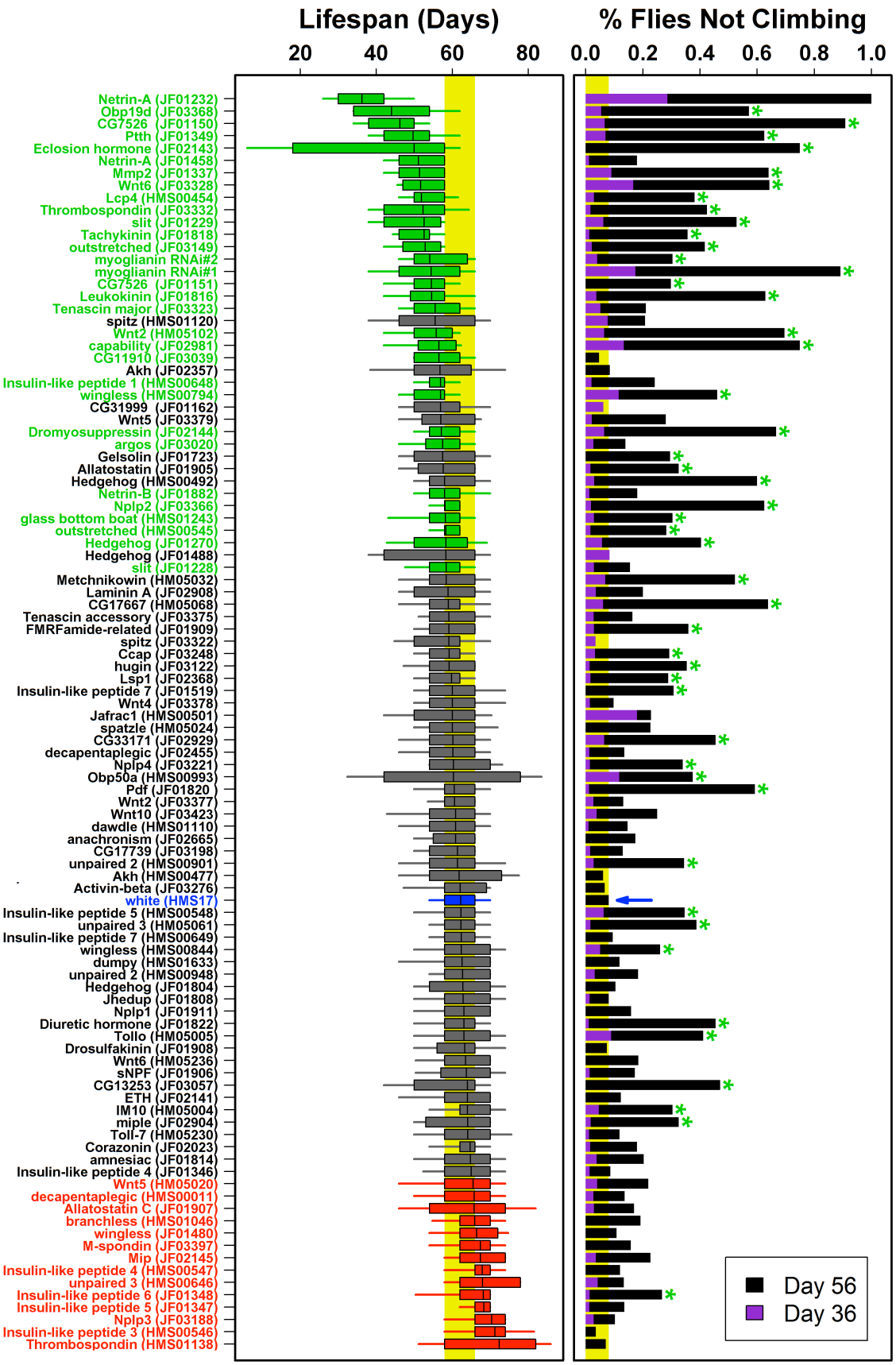
Lifespan (Days)
20
40
60
80
% Flies Not Climbing
0.0
0.2
0.4
0.6
0.8
1.0
Netrin-A (JF01232)
Obp19d (JF03368)
CG7526 (JF01150)
Ptth (JF01349)
Eclosion hormone (JF02143)
Netrin-A (JF01458)
Mmp2 (JF01337)
Wnt6 (JF03328)
Lcp4 (HMS00454)
Thrombospondin (JF03332)
slit (JF01229)
Tachykinin (JF01818)
outstretched (JF03149)
myoglianin RNAi#2
myoglianin RNAi#1
CG7526 (JF01151)
Leukokinin (JF01816)
Tenascin major (JF03323)
spitz (HMS01120)
Wnt2 (HM05102)
capability (JF02981)
CG11910 (JF03039)
Akh (JF02357)
Insulin-like peptide 1 (HMS00648)
wingless (HMS00794)
CG31999 (JF01162)
Wnt5 (JF03379)
Dromyosuppressin (JF02144)
argos (JF03020)
Gelsolin (JF01723)
Allatostatin (JF01905)
Hedgehog (HMS00492)
Netrin-B (JF01882)
Nplp2 (JF03366)
glass bottom boat (HMS01243)
outstretched (HMS00545)
Hedgehog (JF01270)
Hedgehog (JF01488)
slit (JF01228)
Metchnikowin (HM05032)
Laminin A (JF02908)
CG17667 (HM05068)
Tenascin accessory (JF03375)
FMRFamide-related (JF01909)
spitz (JF03322)
Ccap (JF03248)
hugin (JF03122)
Lsp1 (JF02368)
Insulin-like peptide 7 (JF01519)
Wnt4 (JF03378)
Jafrac1 (HMS00501)
spatzle (HM05024)
CG33171 (JF02929)
decapentaplegic (JF02455)
Nplp4 (JF03221)
Obp50a (HMS00993)
Pdf (JF01820)
Wnt2 (JF03377)
Wnt10 (JF03423)
dawdle (HMS01110)
anachronism (JF02665)
CG17739 (JF03198)
unpaired 2 (HMS00901)
Akh (HMS00477)
Activin-beta (JF03276)
white (HMS17)
Insulin-like peptide 5 (HMS00548)
unpaired 3 (HM05061)
Insulin-like peptide 7 (HMS00649)
wingless (HMS00844)
dumpy (HMS01633)
unpaired 2 (HMS00948)
Hedgehog (JF01804)
Jhedup (JF01808)
Nplp1 (JF01911)
Diuretic hormone (JF01822)
Tollo (HM05005)
Drosulfakinin (JF01908)
Wnt6 (HM05236)
sNPF (JF01906)
CG13253 (JF03057)
ETH (JF02141)
IM10 (HM05004)
mipIe (JF02904)
Toll-7 (HM05230)
Corazonin (JF02023)
amnesiac (JF01814)
Insulin-like peptide 4 (JF01346)
Wnt5 (HM05020)
decapentaplegic (HMS00011)
Allatostatin C (JF01907)
branchless (HMS01046)
wingless (JF01480)
M-spondin (JF03397)
Mip (JF02145)
Insulin-like peptide 4 (HMS00547)
unpaired 3 (HMS00646)
Insulin-like peptide 6 (JF01348)
Insulin-like peptide 5 (JF01347)
Nplp3 (JF03188)
Insulin-like peptide 3 (HMS00546)
Thrombospondin (HMS01138)
Day 56
Day 36

Figure S5. Statistical Analysis of the Myokine RNAi Screen (Ordered by Ascending Median Lifespan), Related to Figure 3. Left panel: Results of the RNAi screen (Figure 3) are ordered by ascending median lifespan with each box outlining the middle 50% of survival times for flies in each RNAi treatment, and whiskers outlining the middle 80% of survival times. RNAi treatments significantly increasing lifespan relative to controls (RNAi against the *white*; HMS17) are represented by red boxes, and treatments significantly decreasing lifespan are represented by green boxes (log-rank test; FDR-adjusted $P<0.05$ with at least a 5% change in median lifespan). The vertical yellow region outlines the middle 50% of survival times in the control treatment (HSM17). Two different RNAi treatments in skeletal muscles against the TGF-β ligand *myoglianin* significantly shortened the median lifespan as compared with RNAi against *white* (HMS17).
Right panel: Percentage of flies with climbing defects at days 36 (violet) and 56 (black). A green asterisk is used to denote cohorts for which the percentage of flies with climbing defects at day 56 is significantly higher than in controls at day 56 (chi-square test; FDR-adjusted $P<0.05$). *Myoglianin* RNAi significantly increases the percentage of flies with climbing defects in old age. None of the RNAi treatments resulted in climbing defects in young age (day 8; Figure 3).

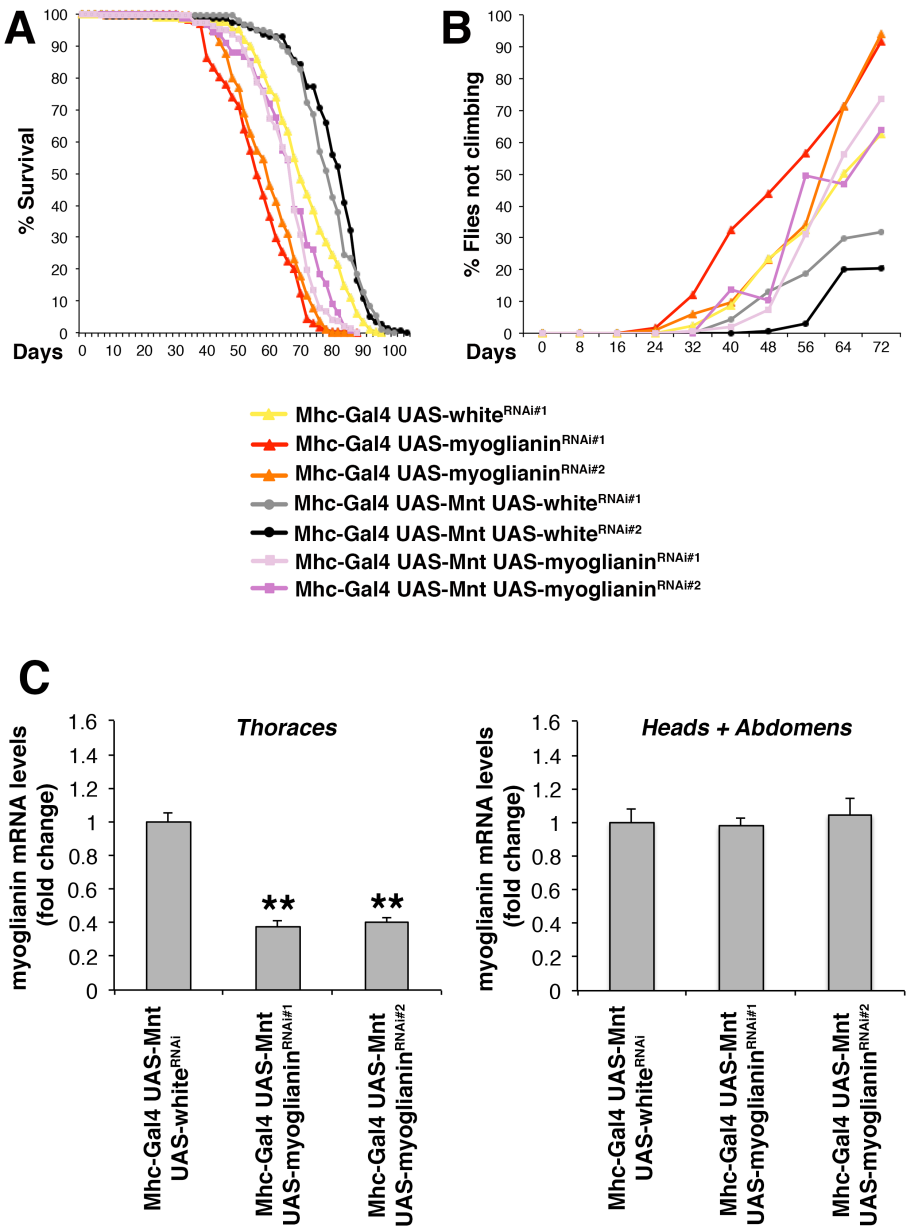

Figure S6. Myoglianin RNAi Leads to Partial Suppression of the Lifespan Extension Induced by Mnt Overexpression in Muscle, Related to Figure 4. (A-B) Overlay of the data shown in Figure 4C-F reporting lifespan and climbing assays. Myoglianin RNAi in Mnt overexpressing muscle is statistically different from Myoglianin RNAi alone, indicating that myoglianin is required only in part for the preservation of climbing ability and lifespan extension induced by Mnt (P<0.001, Log-rank tests). See the legend of Figure 4 for additional information on the statistical analysis of these data. (C) Myoglianin RNAi in muscle overexpressing Mnt results in lower myoglianin mRNA levels in thoraces, which consist mostly of muscle, but not in heads and abdomens, which are enriched in non-muscle tissues. SEM is indicated and n=4. **P<0.01, unpaired two-tailed Student's t-test.

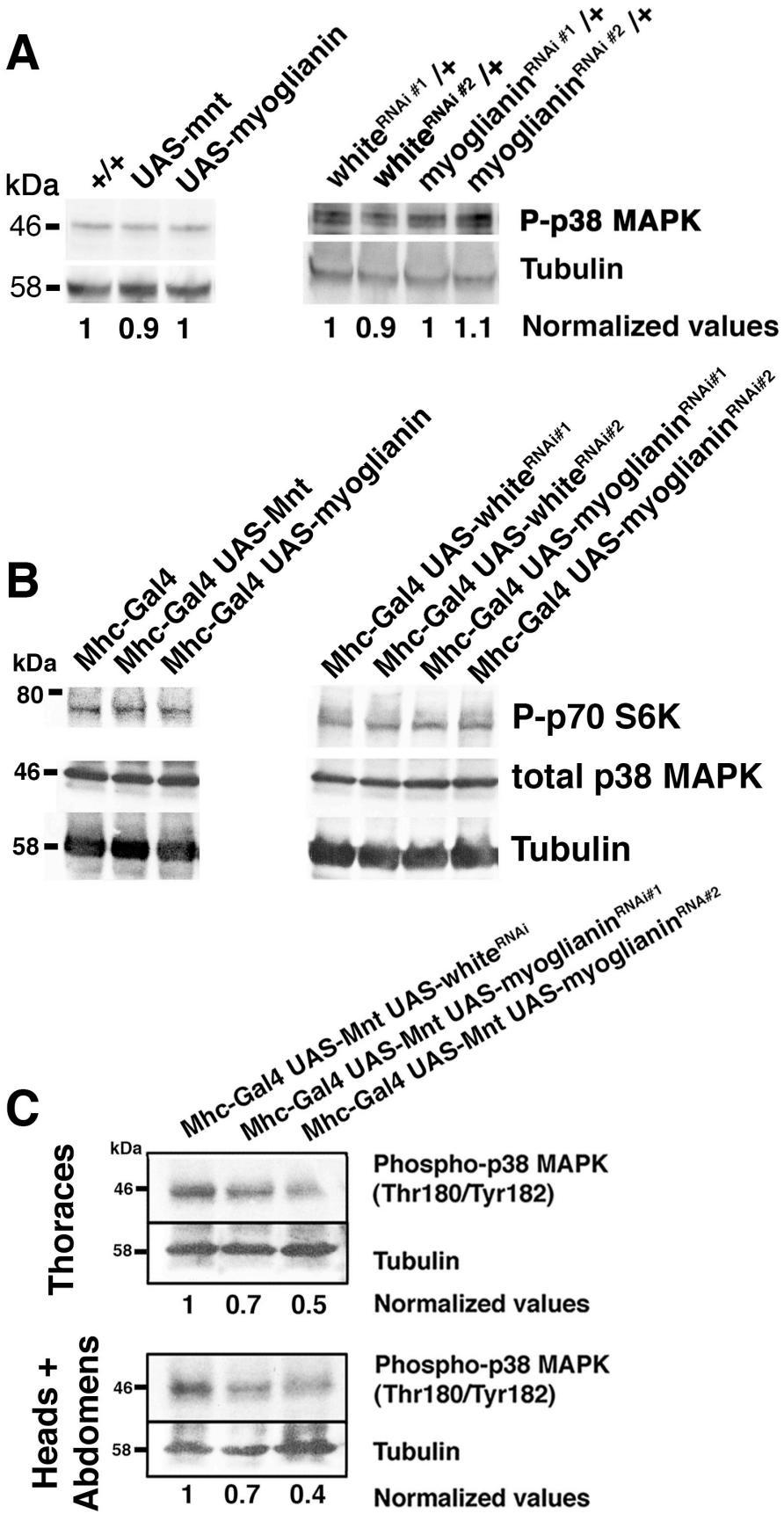
A
+/+
UAS-mnt
UAS-myoglianin
whiteRNAi #1 /+
whiteRNAi #2 /+
myoglianinRNAi #1 /+
myoglianinRNAi #2 /+
kDa
46
58
P-p38 MAPK
Tubulin
1 0.9 1
1 0.9 1 1.1
Normalized values
B
Mhc-Gal4
Mhc-Gal4 UAS-Mnt
Mhc-Gal4 UAS-myoglianin
Mhc-Gal4 UAS-whiteRNAi#1
Mhc-Gal4 UAS-whiteRNAi#2
Mhc-Gal4 UAS-myoglianinRNAi#1
Mhc-Gal4 UAS-myoglianinRNAi#2
kDa
80
46
58
P-p70 S6K
total p38 MAPK
Tubulin
C
Mhc-Gal4 UAS-Mnt UAS-whiteRNAi
Mhc-Gal4 UAS-Mnt UAS-myoglianinRNAi#1
Mhc-Gal4 UAS-Mnt UAS-myoglianinRNA#2
Thoraces
kDa
46
58
Phospho-p38 MAPK
(Thr180/Tyr182)
Tubulin
1 0.7 0.5
Normalized values
Heads +
Abdomens
46
58
Phospho-p38 MAPK
(Thr180/Tyr182)
Tubulin
1 0.7 0.4
Normalized values

Figure S7. Additional Analysis of P-p38 MAPK, total p38 MAPK, and P-p70 S6K levels in Response to Mnt/Myoglianin Signaling, Related to Figure 7.

(A) Absence of changes in P-p38 MAPK levels in UAS-transgene alone controls. Western blot analysis of phospho-p38 (P-p38) MAPK levels in thoraces from heterozygous flies carrying UAS- transgenes but no Mhc-Gal4. Normalization of P-p38 MAPK levels with α-tubulin levels (loading control) indicates the lack of changes in P-p38 MAPK levels in the absence of Gal4-driven transgene expression.

(B) Western blot analysis of phospho-p70 S6K and total p38 MAPK levels in response to *Mnt* and *myoglianin* overexpression and RNAi in muscle. No substantial changes were detected, indicating that Mnt/Myoglianin signaling regulates phosphorylation of p38 MAPK (Figure 7) but not total p38 MAPK protein levels and phospho-p70 S6K levels.

(C) Myoglianin RNAi in muscle overexpressing Mnt results in lower P-p38 MAPK levels in thoraces and heads and abdomens when compared to white RNAi (control). See also Figure 7.

EXTENDED EXPERIMENTAL PROCEDURES

Fly Stocks

The following fly stocks were used: *ppl-Gal4* (Colombani et al., 2003); *Mhc-Gal4* (Schuster et al., 1996); *dMef2-Gal4* (Ranganayakulu et al., 1996), *UAS-Mnt* and *Mnt*$^{1/1}$ (Loo et al., 2005); *UAS-white*^{RNAi} *#1* and *#2* (TRiP ID: HMS0017 and JF01786), *UAS-myoglianin*^{RNAi} *#1* and *#2* (Awasaki et al., 2011), *UAS-RpS3*^{RNAi} (JF01410), *UAS-RpLP0*^{RNAi} (JF01335), *UAS-Nopp140*^{RNAi} (HMS00564), *UAS-eIF-4a*^{RNAi} (HMS00927), *UAS-Brf*^{RNAi} (JF02482), *UAS-Ssrp*^{RNAi} (JF02120), *UAS-CG5033*^{RNAi} (HMS01433), *UAS-p38MAPK WT* (wild-type) and *UAS-p38MAPK KD*^{3} (kinase dead; (Vrailas-Mortimer et al., 2011)). Additional transgenic RNAi stocks used in the screen were from the DRSC/TRiP (http://www.flyrnai.org/TRiP-HOME.html/; (Ni et al., 2009; Ni et al., 2011)) and are indicated in Figures S5.

Construction of *UAS-myoglianin*

To generate *UAS-myoglianin*, the *Drosophila melanogaster myoglianin (CG1838)* coding sequence, corresponding to nucleotides 844-2640 of sequence AY061367, was amplified by PCR using the full-length cDNA clone LD29161 as template with primers 5'-gccagatctatgctggccaactcatgctgcggttgg-3' and 5'-gccctcgagctaagaacag ctgcaaccctcgacagac-3' (underlined are *Bgl*II and *Xho*I restriction sites, respectively). The PCR product was cut with *Bgl*II and *Xho*I for cloning into the pUAST vector, followed by sequencing and injection into *y*^{1}*w*^{1118} embryos.

Capillary Feeding (CAFÉ) Assays

For capillary feeding (CAFÉ) assays (Ja et al., 2007), groups of 10 flies were transferred twelve hours before the assay from standard food to 1.5% agar vials and fed a 5% sucrose solution in PBS provided via a 5 μl calibrated glass micropipette (VWR, #53432-706). At the start of the assay, the old micropipette was replaced with a new one and the amount of liquid food consumed was recorded every 2 hours and corrected on the basis of the evaporation observed in a vial without flies.

Muscle and Body Weight Measurements

For measurement of body weight, 3 groups of 10 flies were weighted on a precision balance and the average body weight calculated. For measurement of thoracic weight (indicative of muscle mass), 3 groups of 10 thoraces were weighted and the average weight calculated.

Immunostaining, Laser Scanning Confocal Microscopy, and Image Analysis

Dissected tissues were fixed for 20 minutes in PBS with 4% paraformaldehyde and 0.1% Triton X-100, washed, and incubated overnight with 1:100 dilution of anti-Fibrillarin (Nop1p; Encore Biotechnology #MCA-38F3) or mouse anti-Mnt (P5D6) (Loo et al., 2005). The following day, samples were washed and

incubated overnight with DAPI (Invitrogen, 1μg/mL), Alexa555-conjugated secondary antibodies (Molecular Probes, 1:200), and Alexa635-conjugated Phalloidin (Molecular Probes, 1:100). Samples were imaged with a Leica SP2 confocal microscope. Image analysis was done with the "Analyze particle" function of ImageJ.

Luciferase Assays

Luciferase assays were done as before (Demontis and Perrimon, 2010). 15×10^4 S2R+ cells/cm^2 were seeded in Schneider's medium (Gibco) containing 10% FCS and transfected one day later using the Effectene Transfection Kit (Qiagen). The following day the medium was changed and, after an additional 3 days in culture, the luciferase assay was performed with the Dual-Glo Luciferase Assay (Promega) according to manufacturer's instructions.

The *CG4364-* and *CG5033-firefly* luciferase reporters were previously described (Hulf et al., 2005). To generate the *myoglianin-Renilla* luciferase reporter, the proximal promoter region (>4:718244,716674) of the *myoglianin* gene (*CG1838*) was amplified by PCR and cloned into the pRL-null vector (Promega) with *Xho*I and *EcoR*I. *UAS-Mnt* and *UAS-YFP* plasmids for overexpression of either *Mnt* (*CG13316*) or *yellow fluorescent protein* (*YFP*) were provided by the DRSC at Harvard Medical School.

In experiments with the *myoglianin-Renilla* luciferase reporter, an *actin-firefly* luciferase reporter was co-transfected as normalization control and luciferase activity refers to ratio of *Renilla* to firefly luciferase activity. In experiments with the *CG4364- and CG5033-firefly* luciferase reporters (Hulf et al., 2005), an *actin-Renilla* luciferase reporter was co-transfected as normalization control and luciferase activity refers to ratio of firefly to *Renilla* luciferase activity. S2R+ cells were also co-transfected with either *UAS-YFP* (control) or *UAS-Mnt* as indicated.

Western Blots

Samples were prepared by homogenizing in a bullet blender (NextAdvance) either fly thoraces (consisting mainly of muscles) or heads and abdomens (consisting mainly of non-muscle tissues) from at least 15 male flies per group in RIPA buffer with protease and phosphatase inhibitors. SDS-PAGE was done as previously (Demontis and Perrimon, 2010). Primary antibodies used are anti-P-p38 MAPK (Cell Signaling Technologies #9215), anti-*Drosophila* P-p70 S6K (Cell Signaling Technologies #9209), anti-total p38 MAPK (Cell Signaling Technologies #9212), and anti-α-Tubulin (Cell Signaling Technologies #2125). For densitometry of Western blots, band intensity was quantified with the Histogram function of Photoshop.

Bioinformatic Analysis

Multiple sequence alignment and phylogenetic analysis were done with ClustalW, available at http://www.ebi.ac.uk/Tools/msa/clustalw2/, and orthology prediction with DIOPT, available at http://www.flyrnai.org/cgi-bin/DRSC_orthologs.pl.

Statistical Analysis
Statistical analysis was performed with Excel and the GraphPad Prism software. Unpaired two-tailed Student's *t*-test was used to compare means of two independent groups to each other, while two-way ANOVA followed by Tukey's post test was used to compare the means of more than two independent groups of normally distributed data. Log-rank tests were employed for the statistical analysis of lifespan data and negative geotaxis assays.

Statistical Analysis of the RNAi Screen
Differences in median lifespan were analyzed using the log-rank test as implemented in the "survdiff" function included within the R package "survival" (Therneau, 2012). Survival times for each RNAi treatment were compared with the control ($white^{RNAi}$; HMS00017). To control the false discovery rate, *P*-values generated from each log-rank test were adjusted by using the Benjamini-Hochberg method (Benjamini Y, 1995). To qualify as a statistically significant difference compared with $white^{RNAi}$, an FDR-adjusted *P*-value of less than 0.05 (log-rank test) was required in addition to at least a 5% difference in median lifespan. Similarly, differences in the percentage of flies with climbing defects at day 56 were analyzed using a chi-square test, as implemented in the function "prop.test" included within the R statistical software, with *P*-values from each test adjusted by using the Benjamini-Hochberg method. For a statistically significant difference in climbing ability compared with $white^{RNAi}$, an FDR-adjusted *P*-value of less than 0.05 (chi-square test) was required.

Statistical Analysis of Microarrays
Genome-wide expression levels were evaluated using the Affymetrix *Drosophila* Genome 2.0 array platform (18,952 probe sets representing transcripts associated with 12,440 unique fly genes). Array hybridizations were performed following standard Affymetrix protocols, yielding CEL files in standard format containing probe-level intensity estimates. Quality control metrics were calculated by using CEL files generated for each array, including average background, scale factor, percent present, RNA degradation score, RLE median, RLE IQR, NUSE median and NUSE IQR (Bolstad BM, 2005). There was no indication of problematic array hybridizations based upon these quality-control metrics. Normalized expression scores were calculated for each array by using robust multichip average (RMA) (Bolstad BM, 2003). Presence and absence calls were calculated by using the Wilcoxon rank sum test, as implemented in the MAS 5.0 algorithm (Liu WM, 2002). Of 18,952 probe sets, 6,353 were identified for which signal intensities were not significantly above background with respect to any of the arrays. These 6,353 probe sets were excluded, leaving a total of 12,599 probe sets for further analyses. Differential expression between treatments was analyzed by using linear models with variance estimates moderated using empirical Bayes methods (Smyth, 2005). Raw *P*-values were generated based upon moderated T statistics generated for each gene and each treatment comparison (Smyth, 2005). To assess significance given the total number of hypotheses evaluated, raw *P*-values were adjusted to control the false discovery

using the Benjamini-Hochberg method (Benjamini Y, 1995). Probe set annotation for the Affymetrix *Drosophila* Genome 2.0 array was obtained from the R Bioconductor package "drosophila2.db" (Carlson M, 2012a). Additional annotation for the *Drosophila* genome was obtained using the package "org.Dm.eg.db" (Carlson M, 2012b).

Overrepresentation of gene ontology (GO) terms among differentially expressed genes was evaluated using a conditional version of the Fisher's exact test (Bolstad BM, 2005; Falcon S, 2007). In this approach, the significance of a GO term is evaluated based on a filtered set of associated genes, which excludes any genes associated with more specific GO terms already known to be overrepresented. This approach serves to reduce redundancy among GO terms identified as significantly overrepresented with respect to a set of differentially expressed genes (Bolstad BM, 2005; Falcon S, 2007). In these analyses, enrichment of GO terms among differentially expressed genes was evaluated relative to a reference set of fly genes, which was filtered to include only those genes associated with the 12,599 probe sets expressed above background levels.

SUPPLEMENTAL REFERENCES

Awasaki, T., Huang, Y., O'Connor, M.B., and Lee, T. (2011). Glia instruct developmental neuronal remodeling through TGF-beta signaling. Nat Neurosci *14*, 821-823.

Benjamini Y, H.Y. (1995). Controlling the false discovery rate: a practical and powerful approach to multiple testing. Journal of the Royal Statistical Society Series, 289-300.

Bolstad BM, C.F., Brettschneider J, Simpson K, Cope L, et al. (2005). Quality assessment of Affymetrix GeneChip Data (New York: Springer).

Bolstad BM, I.R., Astrand M, Speed TP. (2003). A comparison of normalization methods for high density oligonucleotide array data based on variance and bias. Bioinformatics, 185-193.

Carlson M, F.S., Pages H, Li N. (2012a). drosophila2.db: Affymetrix Drosophila Genome 2.0 Array annotation data (chip drosophila2).

Carlson M, F.S., Pages H, Li N. (2012b). org.Dm.eg.db: Genome wide annotation for Fly.

Colombani, J., Raisin, S., Pantalacci, S., Radimerski, T., Montagne, J., and Leopold, P. (2003). A nutrient sensor mechanism controls Drosophila growth. Cell *114*, 739-749.

Demontis, F., and Perrimon, N. (2010). FOXO/4E-BP signaling in Drosophila muscles regulates organism-wide proteostasis during aging. Cell *143*, 813-825.

Falcon S, G.R. (2007). Using GOstats to test gene lists for GO term association. Bioinformatics, 257-258.

Hulf, T., Bellosta, P., Furrer, M., Steiger, D., Svensson, D., Barbour, A., and Gallant, P. (2005). Whole-genome analysis reveals a strong positional bias of conserved dMyc-dependent E-boxes. Mol Cell Biol *25*, 3401-3410.

Ja, W.W., Carvalho, G.B., Mak, E.M., de la Rosa, N.N., Fang, A.Y., Liong, J.C., Brummel, T., and Benzer, S. (2007). Prandiology of Drosophila and the CAFE assay. Proc Natl Acad Sci U S A *104*, 8253-8256.

Liu WM, M.R., Di X, Ryder TB, Hubbell E, Dee S, Webster TA, Harrington CA, Ho MH, Baid J, Smeekens SP (2002). Analysis of high density expression microarrays with signed-rank call algorithms. Bioinformatics *18(12)*, 1593-1599.

Loo, L.W., Secombe, J., Little, J.T., Carlos, L.S., Yost, C., Cheng, P.F., Flynn, E.M., Edgar, B.A., and Eisenman, R.N. (2005). The transcriptional repressor dMnt is a regulator of growth in Drosophila melanogaster. Mol Cell Biol *25*, 7078-7091.

Ni, J.Q., Liu, L.P., Binari, R., Hardy, R., Shim, H.S., Cavallaro, A., Booker, M., Pfeiffer, B.D., Markstein, M., Wang, H.*, et al.* (2009). A Drosophila Resource of Transgenic RNAi Lines for Neurogenetics. Genetics *182*, 1089-1100.

Ni, J.Q., Zhou, R., Czech, B., Liu, L.P., Holderbaum, L., Yang-Zhou, D., Shim, H.S., Tao, R., Handler, D., Karpowicz, P.*, et al.* (2011). A genome-scale shRNA resource for transgenic RNAi in Drosophila. Nat Methods *8*, 405-407.

Ranganayakulu, G., Schulz, R.A., and Olson, E.N. (1996). Wingless signaling induces nautilus expression in the ventral mesoderm of the Drosophila embryo. Dev Biol *176*, 143-148.

Schuster, C.M., Davis, G.W., Fetter, R.D., and Goodman, C.S. (1996). Genetic dissection of structural and functional components of synaptic plasticity. I. Fasciclin II controls synaptic stabilization and growth. Neuron *17*, 641-654.

Smyth, G. (2005). Limma: linear models for microarray data. (New York: Springer).

Therneau, T. (2012). A Package for Survival Analysis in S.

Vrailas-Mortimer, A., del Rivero, T., Mukherjee, S., Nag, S., Gaitanidis, A., Kadas, D., Consoulas, C., Duttaroy, A., and Sanyal, S. (2011). A muscle-specific

p38 MAPK/Mef2/MnSOD pathway regulates stress, motor function, and life span in Drosophila. Dev Cell *21*, 783-795.